Geometric Local Variance Gamma Model

P. Carr and A. Itkin

P. Carr
is a professor in the Tandon School of Engineering at New York University in Brooklyn, NY.
petercarr@nyu.edu

A. Itkin
is a professor in the Tandon School of Engineering at New York University in Brooklyn, NY.
aitkin@nyu.edu

KEY FINDINGS

- An extension of the Local Variance Gamma model is proposed on the basis of the Geometric Brownian motion with drift.
- Three piecewise linear models: the local variance as a function of strike, the local variance as function of log-strike, and the local volatility as a function of strike (so, the local variance is a piecewise quadratic function of strike) are considered.
- For all these new constructions an ODE is derived which replaces the Dupire equation and can be solved in closed form.

ABSTRACT: *This article describes another extension of the local variance gamma model originally proposed by Carr in 2008 and then further elaborated by Carr and Nadtochiy in 2017 and Carr and Itkin in 2018. As compared with the latest version of the model developed by Carr and Itkin and called the "expanded local variance gamma" (ELVG) model, two innovations are provided in this article. First, in all previous articles the model was constructed on the basis of a gamma time-changed arithmetic Brownian motion: with no drift in Carr and Nadtochiy, with drift in Carr and Itkin, and with the local variance a function of the spot level only. In contrast, this article develops a geometric version of this model with drift. Second, in Carr and Nadtochiy the model was calibrated to option smiles assuming that the local variance is a piecewise constant function of strike, while in Carr and Itkin the local variance was assumed to be a piecewise linear function of strike. In this article, the authors consider three piecewise linear models: the local variance as a function of strike, the local variance as a function of log-strike, and the local volatility as a function of strike (so, the local variance is a piecewise quadratic function of strike). The authors show that for all these new constructions, it is still possible to derive an ordinary differential equation for the option price, which plays the role of Dupire's equation for the standard local volatility model, and moreover, it can be solved in closed form. Finally, similar to in Carr and Itkin, the authors show that given multiple smiles the whole local variance/volatility surface can be recovered without requiring solving any optimization problem. Instead, it can be done term-by-term by solving a system of nonlinear algebraic equations for each maturity, which is a significantly faster process.*

TOPICS: ***Derivatives, statistical methods, options****

The local variance gamma (LVG) volatility model was first introduced by P. Carr in 2008 and then presented in Carr and Nadtochiy

*All articles are now categorized by topics and subtopics. **View at PM-Research.com.**

(2014, 2017) as an extension of the local volatility model by Dupire (1994) and Derman and Kani (1994). The latter was developed in addition to the celebrated Black–Scholes model to take into account the existence of option smile. The main advantage of all local volatility models is that given European options prices or their implied volatilities at points (T, K) where K, T are the option strike and time to maturity, they are able to exactly replicate the local volatility function $\sigma(T, K)$ at these points. This process is called "calibration of the local volatility" (or, alternatively, "implied volatility") surface; see survey in Carr and Itkin (2018), Itkin and Lipton (2018), and references therein.

However, as compared with the classical local volatility model, the LVG and the expanded local variance gamma (ELVG) have several advantages. First, they are richer in the financial sense. Indeed, it is worth noting that the term "local" in the name of the LVG/ELVG models is a bit confusing. For example, the ELVG is constructed by equipping an arithmetic Brownian motion with drift and local volatility by stochastic time change $\Gamma_{X(t)}$. Here Γ_t is a gamma stochastic variable, and $X(t)$ is a deterministic function of time t. As stochastic change is one of the ways of introducing stochastic volatility, it could be observed that the LVG and ELVG models are actually local stochastic volatility (LSV) models that combine local and stochastic features of the volatility process. For more information on the LSV models, see Bergomi (2016) and Kienitz and Wetterau (2012).

Another advantage of the LVG and ELVG models is that their calibration is computationally more efficient. The reason being this construction gives rise not to a partial differential equation (which in the classical case is known as Dupire's equation), but to a partial divided-difference equation (PDDE). The latter is actually an ordinary differential equation (ODE) and permits both explicit calibration and fast numerical valuation. In particular, calibration of the local variance surface does not require any optimization method, rather just a root solver (Carr and Itkin 2018).

As discussed in Itkin and Lipton (2018), given the market quotes of European options for various maturities and strikes, the local (and then implied) volatility surface can be obtained by directly solving the Dupire equation using either analytical or numerical methods. The advantage of such an approach is that it guarantees no-arbitrage if the corresponding analytical or numerical method does preserve no-arbitrage (including various interpolations, etc.). Obviously, solving Dupire's partial differential equation (PDE) requires either numerical methods, for example, those in Coleman, Kim, Li, and Verma (2001) or, as in Itkin and Lipton (2018), a semi-analytic method that (1) first uses the Laplace–Carson transform and (2) then applies various transformations to obtain a closed form solution of the transformed equation in terms of Kummer hypergeometric functions. Still, it requires an inverse Laplace transform to obtain the final solution. To make the second approach tractable, some assumptions should be made about the behavior of the local/implied volatility surface at strikes and maturities for which the market quotes are not known. Usually, the corresponding local variance is assumed to be piecewise constant, Lipton and Sepp (2011), or piecewise linear, Itkin and Lipton (2018), in the log-strike space, and piecewise constant in the time-to-maturity space. A similar assumption is also necessary to make the LVG/ELVG models tractable. In particular, in Carr and Nadtochiy (2017) the model was calibrated to option smiles assuming the local variance is a *piecewise constant* function of strike, while in Carr and Itkin (2018) the local variance is assumed to be a *piecewise linear* function of strike.

Despite these nice features of the ELVG, one possible problem could be that the model is developed according to the arithmetic Brownian motion with drift. That means that the underlying, in principle, could acquire negative values, which in some cases is undesirable, for example if the underlying is a stock price. Therefore, in this article we describe another extension of the LVG model, which operates with a gamma time-changed *geometric* Brownian motion with drift, and the local variance, which is a function of the spot level only (so is not a function of time).

Second, in Carr and Nadtochiy (2017), the model was calibrated to option smiles assuming the local variance is a *piecewise constant* function of strike, while in Carr and Itkin (2018) the local variance is assumed to be a *piecewise linear* function of strike. In this article we consider three *piecewise linear* models: the local variance as a function of strike, the local variance as a function of log-strike, and the local volatility as a function of strike (so, the local variance is a *piecewise quadratic* function of strike). We show that in this new model it is still possible to derive an ODE for the option price, which plays a role in the Dupire equation for the standard local volatility model. Moreover, in all three cases, this equation can be solved in closed form. Finally, similar

to Carr and Itkin (2018), we show that given multiple smiles, the whole local variance/volatility surface can be recovered without having to solve any optimization problem. Instead, it can be done term-by-term, and for every maturity the entire calibration is done by solving a system of nonlinear algebraic equations, which is a significantly faster process.

The rest of this article is organized as follows. In the following section we formulate the new model, which for an obvious reason we call the geometric local variance gamma (or GLVG) model. Then we derive a forward equation, which is an ODE, for put option prices using a homogeneous Bochner subordination approach. The next section, on piecewise models of local variance/volatility, generalizes this approach by considering the local variance being piecewise constant in time. A closed form solution of the derived ODE is given in terms of hypergeometric functions for various models of the local variance or volatility. The next section discusses computation of a source term of this ODE that requires a no-arbitrage interpolation. Using the idea of Itkin and Lipton (2018), we show how to construct nonlinear interpolation, which provides both no-arbitrage and a nice tractable representation of the source term, so that all integrals in the source term can be computed in closed form. The calibration of multiple smiles in our model is then discussed in detail. To calibrate a single smile we derive a system of nonlinear algebraic equations for the model parameters and explain how to obtain a smart guess for their initial values. Next, we discuss the results of some numerical experiments in which calibration of the model to the given market smiles is done term-by-term. Conclusions are presented in the final section.

STOCHASTIC MODEL

Let W_t be a $\mathbb{Q}$ standard Brownian motion with time index $t \geq 0$. Consider a stochastic process D_t to be a time-homogeneous diffusion with drift μ

$$dD_t = \mu D_t dt + \sigma(D_t) D_t dW_t, \tag{1}$$

where the volatility function σ is local and time-homogeneous.

A unique solution to Equation 1 exists if $\sigma(D)$: $\mathbb{R} \to \mathbb{R}$ is Lipschitz continuous in D and satisfies growth conditions at infinity. Since D is a time-homogeneous Markov process, its infinitesimal generator $\mathcal{A}$ is given by

$$\mathcal{A}\phi(D) \equiv \left[\mu D \nabla_D + \frac{1}{2}\sigma^2(D) D^2 \nabla_D^2 \right] \phi(D) \tag{2}$$

for all twice differentiable functions ϕ. Here ∇_x is a first order differential operator on x (the first derivative). The semigroup of the D process (which here is an expectation under $\mathbb{Q}$) is

$$\mathcal{T}_t^D \phi(D_t) = e^{t\mathcal{A}} \phi(D_t) = \mathbb{E}_{\mathbb{Q}}[\phi(D_t) | D_0 = D], \ \forall t \geq 0. \tag{3}$$

This first equality could also be thought of as the Feynman–Kac theorem representation of the solution to the terminal value problem (see, for example, Lörinczi, Hiroshima, and Betz 2011), which connects the expectation in the right-hand side (RHS) to the solution of the corresponding PDE, and then the formal solution of this PDE is given by the exponential operator $e^{t\mathcal{A}}$ applied to the initial condition $\phi(D_t)$.

In the spirit of Carr and Nadtochiy (2017), Carr and Itkin (2018) introduce a new process D_{Γ_t}, which is D_t subordinated by the unbiased gamma clock Γ_t. The density of the unbiased gamma clock Γ_t at time $t \geq 0$ is

$$\mathbb{Q}\{\Gamma_t \in d\nu\} = \frac{\nu^{m-1} e^{-\nu m/t}}{(t^*)^m \Gamma(m)} d\nu, \quad \nu > 0, \quad m \equiv t/t^*. \tag{4}$$

Here $t^* > 0$ is a free parameter of the process, and $\Gamma(x)$ is the gamma function. It is easy to check that

$$\mathbb{E}_{\mathbb{Q}}[\Gamma_t] = t. \tag{5}$$

Thus, on average the stochastic gamma clock Γ_t runs synchronously with the calendar time t.

As applied to the option pricing problem, we introduce a more complex construction. Namely, consider options written on the underlying process S_t. Without loss of generality and for the sake of clearness, let us treat S_t below as the stock price process. Let us define S_t as

$$S_t = D_{\Gamma_{X(t)}} \tag{6}$$

where $X(t)$ is a deterministic function of time t. We need to determine $X(t)$ such that under a risk-neutral measure $\mathbb{Q}$, the total gains process $\hat{S}_t$, including the underlying price appreciation and continuous dividends q,

after discounting at the risk-free rate r, is a martingale (see Shreve 1992).

Taking first a derivative of $\hat{S}_t$

$$d\hat{S}_t = d(e^{-rt}S_t e^{qt}) = e^{(q-r)t}[(q-r)S_t dt + dS_t], \tag{7}$$

and then an expectation of both parts, we obtain

$$\mathbb{E}_{\mathbb{Q}}[d(e^{(q-r)t}S_t)] = e^{(q-r)t}\{(q-r)\mathbb{E}_{\mathbb{Q}}[S_t]dt + d\mathbb{E}_{\mathbb{Q}}[S_t]\}. \tag{8}$$

So, for $\hat{S}_t$ to be a martingale, the RHS of Equation 8 should vanish. Solving the equation

$$(q-r)\gamma(t)dt + d\gamma(t) = 0, \qquad \gamma(t) = \mathbb{E}_{\mathbb{Q}}[S_t|S_s],\ s < t$$

we obtain

$$\gamma(t) = \mathbb{E}_{\mathbb{Q}}[S_t|S_s] = S_s e^{(r-q)(t-s)},$$
$$\mathbb{E}_{\mathbb{Q}}[dS_t|S_s] = d\mathbb{E}_{\mathbb{Q}}[S_t|S_s] = S_s(r-q)e^{(r-q)(t-s)}dt. \tag{9}$$

However, from Equation 6

$$\begin{aligned}\mathbb{E}_{\mathbb{Q}}[dS_t|S_s] &= \mathbb{E}_{\mathbb{Q}}[dD_{\Gamma_{X(t)}}|S_s] = \mu\mathbb{E}_{\mathbb{Q}}[D_{\Gamma_{X(t)}}d\Gamma_{X(t)}|S_s] \\ &\quad + \mathbb{E}_{\mathbb{Q}}[\sigma(D_{\Gamma_{X(t)}})D_{\Gamma_{X(t)}}dW_{\Gamma_{X(t)}}|S_s] \\ &= \mu\mathbb{E}_{\mathbb{Q}}[D_{\Gamma_{X(t)}}d\Gamma_{X(t)}|S_s]\end{aligned} \tag{10}$$

because the process $W_{\Gamma_{X(t)}}$ is a local martingale (see Revuz and Yor 1999, chapter 6). Accordingly, the process $W_{\Gamma_{X(t)}}$ inherits this property from W_{Γ_t}; hence $\mathbb{E}_{\mathbb{Q}}[\sigma(D_{\Gamma_{X(t)}})D_{\Gamma_{X(t)}}dW_{\Gamma_{X(t)}}] = 0$.

To proceed, assume the gamma process Γ_t is independent of W_t (and, accordingly, $\Gamma_{X(t)}$ is independent of $W_{\Gamma_{X(t)}}$). Then the expectation in the RHS of Equation 10 can be computed by first conditioning on $\Gamma_{X(t)}$ and then integrating over the distribution of $\Gamma_{X(t)}$, which can be obtained from Equation 4 by replacing t with $X(t)$, that is,

$$\begin{aligned}&\mathbb{E}_{\mathbb{Q}}[D_{\Gamma_{X(t)}}d\Gamma_{X(t)}|S_s] \\ &= \int_0^\infty \mathbb{E}_{\mathbb{Q}}[D_{\Gamma_{X(t)}}d\Gamma_{X(t)}|\Gamma_{X(t)} = \nu]\frac{\nu^{m-1}e^{-\nu m/X(t)}}{(t^*)^m\Gamma(m)} \\ &= \int_0^\infty \mathbb{E}_{\mathbb{Q}}[D_\nu]\frac{\nu^{m-1}e^{-\nu m/X(t)}}{(t^*)^m\Gamma(m)}d\nu, \quad \nu > 0, \quad m \equiv X(t)/t^*.\end{aligned} \tag{11}$$

To find $\mathbb{E}_{\mathbb{Q}}[D_\nu]$ we take into account Equation 1 to obtain

$$\begin{aligned}d\mathbb{E}_{\mathbb{Q}}[D_\nu] &= \mathbb{E}_{\mathbb{Q}}[dD_\nu] \\ &= \mathbb{E}_{\mathbb{Q}}[\mu D_\nu d\nu + \sigma(D_\nu)D_\nu dW_\nu] \\ &= \mu\mathbb{E}_{\mathbb{Q}}[D_\nu]d\nu.\end{aligned} \tag{12}$$

Solving this equation with respect to $\gamma(\nu) = \mathbb{E}_{\mathbb{Q}}[D_\nu|D_s]$, we obtain $\mathbb{E}_{\mathbb{Q}}[D_\nu|D_s] = D_s e^{\mu(\nu-s)}$. Since we condition on time s, it means that $D_s = D_{\Gamma_{X(s)}} = S_s$, and thus $\mathbb{E}_{\mathbb{Q}}[D_\nu|D_s] = S_s e^{\mu(\nu-s)}$.

Further, we substitute this into Equation 11, set the parameter of the gamma distribution t^* to be $t^* = X(t)$ (so $m = 1$), and integrate to obtain

$$\mathbb{E}_{\mathbb{Q}}[dS_t|S_s] = \mu\mathbb{E}_{\mathbb{Q}}[D_{\Gamma_{X(t)}}d\Gamma_{X(t)}] = S_s e^{-s\mu}\frac{\mu}{1-\mu X(t)}dt. \tag{13}$$

Finally, equating representations of $\mathbb{E}_{\mathbb{Q}}[dS_t|S_s]$ obtained in Equation 9 and Equation 13 we arrive at the equation for $X(t)$:

$$S_0(r-q)e^{(r-q)(t-s)} = S_s e^{-s\mu}\frac{\mu}{1-\mu X(t)}. \tag{14}$$

Assuming $\mu = r - q$, this equation can be solved to provide

$$X(t) = \frac{1-e^{-(r-q)t}}{r-q}. \tag{15}$$

This expression for $X(t)$ was also used in Carr and Itkin (2018) for the ELVG. We previously mentioned that the ELVG could be considered as an *arithmetic analog* of our model in this article, which is *geometric* in D_t.

It is clear that in the limit $r \to 0$, $q \to 0$, we have $X(t) = t$. Also based on Equation 5,

$$\mathbb{E}_{\mathbb{Q}}[\Gamma_{X(t)}] = X(t). \tag{16}$$

The function $X(t)$ starts at zero, that is, $X(0) = 0$,[1] and is a continuous nondecreasing function of time t. In more detail, if $r - q > 0$, the function $X(t)$ is increasing in t in all points except at $t \to \infty$, where it tends to be constant. However, the infinite time horizon does not

[1] So our assumption made above that $X(0) = 0$ is consistent.

have much practical sense; therefore, for any finite time t the function $X(t)$ can be treated as an increasing function in t. In the other case, when $r - q < 0$, the function $X(t)$ is strictly increasing $\forall t \in [0, \infty)$. This means that, overall, $X(t)$ has all the properties of a good clock. Accordingly, $\Gamma_{X(t)}$ has all the properties of a random time.

Thus, we managed to demonstrate that with this choice of μ and $X(t)$, the right-hand part of Equation 8 vanishes, and our discounted stock process with allowance for non-zero interest rates and continuous dividends becomes a martingale. So the proposed construction can be used for option pricing.

This setting can be easily generalized for time-dependent interest rates $r(t)$ and continuous dividends $q(t)$. We leave that for the reader.

The next step is to establish a connection between the original and time-changed processes. It is known from Bochner (1949) that the process G_t defined as

$$dG_t = \sigma^2(G)G_t dW_t$$

is a time-homogeneous Markov process. The same is true for the process $(r - q)G_t dt$. Thus, the entire process D_t defined in Equation 1 is also a time-homogeneous Markov process. Accordingly, the semigroups $\mathcal{T}_t^S$ of S_t and $\mathcal{T}_t^D$ of D_t are connected by the Bochner integral,[2]

$$\mathcal{T}_t^S U(S) = \int_0^\infty \mathcal{T}_\nu^D U(S)\mathbb{Q}\{\Gamma_{X(t)} \in d\nu\}, \quad \forall t \geq 0, \quad (17)$$

where $U(S)$ is a function in the domain of $\mathcal{T}_t^D$ and $\mathcal{T}_t^S$. It can be derived by exploiting the time homogeneity of the D process, conditioning on the gamma time first and taking into account the independence of Γ_t and W_t (or $\Gamma_{\Gamma_{x(t)}}$ and $W_{\Gamma_{x(t)}}$, in our case).

As we set parameter $t*$ of the gamma clock to $t* = X(t)$, Equation 17 and Equation 4 imply

$$\mathcal{T}_t^S U(S) = \int_0^\infty \mathcal{T}_\nu^D U(S)\frac{e^{-\nu/X(t)}}{X(t)}d\nu. \quad (18)$$

In what follows, for the sake of brevity, we call this model the "geometric local variance gamma model," or the GLVG.

[2] Here it represents an expectation of the option price with respect to the second stochastic driver—stochastic clock ν.

FORWARD EQUATION FOR OPTION PRICES

In this section we derive a forward equation for put option prices, which is an analog of the Dupire equation for the standard local volatility model. In doing so, we closely follow the description in the corresponding section of Carr and Itkin (2018), as from the derivation point of view, the GLVG differs from the ELVG just by the definition of infinitesimal generator $\mathcal{A}$ of the process D_t.

Let us interpret the index t of the semigroup $\mathcal{T}_t^S$ as the maturity date T of a European claim with the valuation time $t_v = 0$. Also let the test function $U(S)$ be the payoff of this European claim, that is,

$$U(S_T) = e^{-rT}(K - S_T)^+. \quad (19)$$

Then define

$$P(S_0, T, K) = \mathcal{T}_T^S U(S_0) \quad (20)$$

as the European put value with maturity T at time $t = 0$ in the GLVG model. Similarly

$$P^D(S_0, \nu, K) = \mathcal{T}_\nu^D U(S_0) \quad (21)$$

would be the European put value with maturity ν at time $t = 0$ in the model of Equation 1.[3] Then the Bochner integral in Equation 18 takes the form

$$P(S, T, K) = \int_0^\infty P^D(S, \nu, K)pe^{-p\nu}d\nu, \quad p \equiv 1/X(T). \quad (22)$$

Thus, $P(S, T, K)$ is represented by a Laplace–Carson transform of $P^D(S, \nu, K)$ with p being the transform parameter. Note that

$$P(S, 0, K) = P^D(S, 0, K) = U(S). \quad (23)$$

To proceed, we need an analog of the Dupire forward PDE for $P^D(S, \nu, K)$.

Dupire-like Forward PDE

Although this can be done in many different ways, below for the sake of compatibility we do it in the spirit of Carr and Nadtochiy (2017).

[3] Below, for simplicity of notation, we drop the subscript "0" in S_0.

First, differentiating Equation 21 by ν with allowance for Equation 3 yields

$$\begin{aligned}\nabla_\nu P^D(S,\nu,K) &= e^{-r\nu}e^{\nu\mathcal{A}}[\mathcal{A}-r]U(S)\\ &= e^{-r\nu}\mathbb{E}_{\mathbb{Q}}[\mathcal{A}-r]U(S).\end{aligned} \tag{24}$$

We take into account the definition of the generator $\mathcal{A}$ in Equation 2 and also recall that at $t = 0$ we have $D_0 = S_0 \equiv S$. Then Equation 24 transforms to

$$\begin{aligned}\nabla_\nu P^D(S,\nu,K) &= -rP^D(S,\nu,K)\\ &\quad + (r-q)S\nabla_S P^D(S,\nu,K)\\ &\quad + e^{-r\nu}\frac{1}{2}\mathbb{E}_{\mathbb{Q}}[\sigma^2(S)S^2\nabla_S^2 U(S)].\end{aligned} \tag{25}$$

However, we need to express the forward equation using a pair of independent variables (ν, K) while Equation 24 is derived in terms of (ν, S). To do this, observe that

$$\begin{aligned}\mathbb{E}_{\mathbb{Q}}[\sigma^2(S)S^2\nabla_S^2 U(S)] &= \mathbb{E}_{\mathbb{Q}}[\sigma^2(S)S^2\delta(K-S)]\\ &= \mathbb{E}_{\mathbb{Q}}[\sigma^2(K)K^2\delta(K-S)]\\ &= \mathbb{E}_{\mathbb{Q}}[\sigma^2(K)K^2\nabla_K^2 U(S)]\\ &= e^{r\nu}\sigma^2(K)\nabla_K^2 P^D(S,\nu,K).\end{aligned} \tag{26}$$

where the sifting property of the Dirac delta function $\delta(S-K)$ has been used. Also

$$\begin{aligned}&-rP^D(S,\nu,K)+(r-q)S\nabla_S P^D(S,\nu,K)\\ &= e^{-r\nu}\mathbb{E}_{\mathbb{Q}}\left[-r(K-S)^+ + (r-q)S\frac{\partial(K-S)^+}{\partial S}\right]\\ &= e^{-r\nu}\mathbb{E}_{\mathbb{Q}}\left[\begin{array}{l}-r(K-S)^+ - (r-q)(K-S)\dfrac{\partial(K-S)^+}{\partial S}\\ \qquad + (r-q)K\dfrac{\partial(K-S)^+}{\partial S}\end{array}\right]\\ &= e^{-r\nu}\mathbb{E}_{\mathbb{Q}}\left[\begin{array}{l}-r(K-S)^+ + (r-q)(K-S)^+\\ \qquad -(r-q)K\dfrac{\partial(K-S)^+}{\partial K}\end{array}\right]\\ &= -qP^D(S,\nu,K)-(r-q)K\nabla_K P^D(S,\nu,K).\end{aligned} \tag{27}$$

Therefore, using Equations 26 and 27, Equation 24 could be transformed to

$$\begin{aligned}\nabla_\nu P^D(S,\nu,K) &= -qP^D(S,\nu,K)-(r-q)K\nabla_K P^D(S,\nu,K)\\ &\quad + \frac{1}{2}\sigma^2(K)K^2\nabla_K^2 P^D(S,\nu,K)\\ &\equiv \mathcal{A}^K P^D(S,\nu,K),\ \mathcal{A}^K = -q-(r-q)K\nabla_K\\ &\quad + \frac{1}{2}\sigma^2(K)K^2\nabla_K^2.\end{aligned} \tag{28}$$

This equation looks exactly like the Dupire equation with non-zero interest rates and continuous dividends (see, for example, Ekström and Tysk 2012 and references therein). Note, that $\mathcal{A}^K$ is also a time-homogeneous generator.

PDDE for a Single Term

Our final step is to apply the linear differential operator $\mathcal{L}$ defined in Equation 28 to both parts of Equation 22. Using time-homogeneity of D_t and again the Dupire equation, Equation 28, we obtain

$$\begin{aligned}&-qP(S,T,K)-(r-q)K\nabla_K P(S,T,K)\\ &\qquad + \frac{1}{2}\sigma^2(K)K^2\nabla_K^2 P(S,T,K)\\ &= \int_0^\infty pe^{-p\nu}\left[\begin{array}{c}-qP^D(S,\nu,K)-(r-q)K\nabla_K P^D(S,\nu,K)\\ + \dfrac{1}{2}\sigma^2(K)K^2\nabla_K^2 P^D(S,\nu,K)\end{array}\right]d\nu\\ &= \int_0^\infty pe^{-p\nu}\nabla_\nu P^D(S,\nu,K)d\nu = -pP^D(S,0,K)\\ &\quad + p\int_0^\infty P^D(S,\nu,K)pe^{-p\nu}d\nu\\ &= p[P(S,T,K)-P^D(S,0,K)]\\ &= p[P(S,T,K)-P(S,0,K)],\end{aligned} \tag{29}$$

where in the last line we took into account Equation 23.

Thus, finally $P(S, T, K)$ solves the following problem:

$$\begin{aligned}&-qP(S,T,K)-(r-q)K\nabla_K P(S,T,K)\\ &\quad + \frac{1}{2}\sigma^2(K)K^2\nabla_K^2 P(S,T,K)\\ &= \frac{P(S,T,K)-P(S,0,K)}{X(T)},\ P(S,0,K)=(K-S)^+.\end{aligned} \tag{30}$$

In contrast to the Dupire equation, which belongs to the PDE class, Equation 30 is an ODE, or more

precisely a partial divided-difference equation (PDDE), since the derivative in time in the right-hand part is now replaced by a divided difference. In the form of an ODE, it reads

$$\left[\begin{array}{c}\frac{1}{2}\sigma^2(K)K^2\nabla_K^2-(r-q)K\nabla_K \\ -\left(q+\frac{1}{X(T)}\right)\end{array}\right]P(S,T,K)=-\frac{P(S,0,K)}{X(T)}. \tag{31}$$

This equation could be solved analytically for some particular form of the local volatility function $\sigma(K)$, which is considered in the next section. Also in the same way a similar equation could be derived for the call option price $C_0(S, T, K)$, which reads

$$\left[\begin{array}{c}\frac{1}{2}\sigma^2(K)K^2\nabla_K^2+(r-q)K\nabla_K \\ -\left(q+\frac{1}{X(T)}\right)\end{array}\right]C_0(S,T,K)=-\frac{C_0(S,0,K)}{X(T)},$$
$$C_0(S,0,K)=(S-K)^+. \tag{32}$$

Solving Equation 31 or Equation 32 provides the way to determine $\sigma(K)$ given market quotes of call and put options with maturity T. However, this method allows the calibration of just a single term. Calibration of the entire local volatility surface, in principle, could be done term-by-term (because of the time-homogeneity assumption) if Equation 31 and Equation 32 could be generalized to this case.

PDDE for Multiple Terms

This generalization can be done in the same way as presented in Carr and Itkin (2018, section 4). Therefore, we refer the reader to that section while here we provide just some useful comments.

To address the calibration of multiple smiles we need to relax the assumption about time-homogeneity of the D_t process defined in Equation 1. We assume that the local variance $\sigma(D_t)$ is no longer time-homogeneous, but a piecewise constant function of time $\sigma(D_t, t)$.

Let $T_1, T_2, \ldots, T_M$ be the time points at which the variance rate $\sigma^2(D_t)$ jumps deterministically. In other words, at the interval $t \in [T_0, T_1)$, the variance rate is $\sigma_0^2(D_t)$, at $t \in [T_1, T_2)$, it is $\sigma_1^2(D_t)$; and so on. This can be also represented as

$$\sigma^2(D_t,t)=\sum_{i=0}^{M}\sigma_i^2(D_t)w_i(t),$$
$$w_i(t)\equiv \mathbf{1}_{t-T_i}-\mathbf{1}_{t-T_{i+1}},\ i=0,\ldots,M,\quad T_0=0, T_{M+1}=\infty,$$
$$\mathbf{1}_x=\begin{cases}1, & x\geq 0\\ 0, & x<0.\end{cases} \tag{33}$$

Note, that

$$\sum_{i=0}^{M}w_i(t)=\mathbf{1}_t-\mathbf{1}_{t-\infty}=1,\quad \forall t\geq 0.$$

Therefore, in the case in which all $\sigma_i^2(D_t)$ are equal, that is, independent on index i, Equation 33 reduces to the case considered in the previous sections.

The implication is that the volatility $\sigma(D_t)$ jumps as a function of time at the calendar times $T_0, T_1, \ldots, T_M$, and not at the business times ν determined by the gamma clock. Otherwise, the volatility function would have been changed at random (business) times, which means it is stochastic. But this definitely lies outside the scope of our model. Therefore, we need to change Equation 33 to

$$\sigma^2(D_t,t)=\sum_{i=0}^{M}\sigma_i^2(D)\bar{w}_i(\mathbb{E}_{\mathbb{Q}}(t)), \tag{34}$$

$$\bar{w}_i(\mathbb{E}_{\mathbb{Q}}(t))=\mathbf{1}_{X^{-1}(t-T_i)}-\mathbf{1}_{X^{-1}(t-T_{i+1})},\ i=0,\ldots,M,$$
$$X^{-1}(t)=\frac{1}{q-r}\log[1-(r-q)t]. \tag{35}$$

As per the last line, $X(t)$ exists $\forall t \geq 0$ if $q > r$, and $\forall t < 1/(r-q)$ if $r > q$.

Hence, when using Equation 6 we have

$$\sigma^2(D_t,t)|_{t=\Gamma_{X(t)}}=\sum_{i=0}^{M}\sigma_i^2(D)\bar{w}_i(X(t))=\sum_{i=0}^{M}\sigma_i^2(D)w_i(t). \tag{36}$$

Accordingly, if the calendar time t belongs to the interval $T_0 \leq t < T_1$, the infinitesimal generator $\mathcal{A}$ of the semigroup $\mathcal{T}_\nu^D$ is a function of $\sigma(D_t)$, and not of $\sigma(D_\nu)$. As at $T_0 \leq t < T_1$ we assume $\sigma(D) = \sigma_0(D)$, that

is, is constant in time, it does not depend on ν. Thus, $\mathcal{A}$ (which for this interval of time we will denote as $\mathcal{A}_0$) is still time-homogeneous.

Similarly, one can see that for $T_1 \le t < T_2$, the infinitesimal generator $\mathcal{A}_1$ of the semigroup $\mathcal{T}_\nu^D$ is also time-homogeneous and depends on $\sigma_1(D)$, and so on.

Further, similar to Carr and Itkin (2018) it could be shown that the forward partial divided difference equation for the put price $P(S, T_i, K)$, $i = 1, \ldots, M$ reads

$$\left[\frac{1}{2}\sigma^2(K)K^2\nabla_K^2 - (r-q)K\nabla_K - \left(q + \frac{1}{X(T_i) - X(T_{i-1})}\right)\right] P(S,T_i,K) = -\frac{P(S,T_{i-1},K)}{X(T_i) - X(T_{i-1})}. \quad (37)$$

Here the local variance function $\sigma^2(K) = \sigma_i^2(K)$ as it corresponds to the interval $(T_{i-1}, T_i]$, where the above ODE is solved.

Equation 37 is a recurrent equation that can be solved for all $i = 1, \ldots, M$ sequentially starting with $i = 1$ subject to some boundary conditions.

Boundary Conditions

In many financial models in which the dynamics of the stock price are represented by a geometric Brownian motion (perhaps with local or stochastic volatility), for instance, the celebrated Black–Scholes model, the boundary condition at $K \to \infty$ is set to be

$$P(S,T_i,K) \to \mathcal{D}_i K - \mathcal{Q}_i S, \quad K \to \infty,$$

where $\mathcal{D}_i = e^{-rT_i}$ is the discount factor, and $\mathcal{Q}_i = e^{-qT_i}$. Indeed, as it could be easily checked, this condition is a valid solution of the Dupire forward equation, Equation 28, and also reflects the fact that at $K \to \infty$, the put option price should be linear in K. However, this boundary condition does not solve Equation 31, so it could not be used in our model.

Therefore, we propose to set up the boundary condition at $K \to \infty$ by still assuming it to be a linear function of K of the form

$$\lim_{K\to\infty} P(S,T,K) = A(T)K - B(T)S, \quad (38)$$

where $A(T)$ and $B(T)$ are some functions of maturity T to be determined, so the expression in Equation 38 solves Equation 31.

Obviously, $T_0 = 0$ implies $A(T_0) = B(T_0) = 1$. Then we can proceed recursively. For the next given maturity $T = T_1$, by plugging Equation 38 into Equation 37, we obtain at $K \to \infty$

$$\begin{aligned} &-(r-q)KA(T_1)p_1 - (p_1q+1)(A(T_1)K - B(T_1)S) \\ &= -P(S,T_0,K), P(S,T_0,K) = A(T_0)K - B(T_0)S \\ &= K - S, p_j = X(T_j) - X(T_{j-1}) > 0. \qquad j = 1, \ldots, M \end{aligned} \quad (39)$$

From these equations we obtain

$$B(T_1) = \frac{1}{p_1q+1}, \qquad A(T_1) = \frac{1}{p_1r+1}. \quad (40)$$

So in this case $A(T_1)$, $B(T_1)$ are an analog of some kind of discrete compounding.

Proceeding recursively, we derive a general relationship

$$\begin{aligned} B(T_i) &= \frac{B(T_{i-1})}{p_iq+1} = \frac{1}{\prod_{k=1}^{i}(p_iq+1)}, \\ A(T_i) &= \frac{A(T_{i-1})}{p_ir+1} = \frac{1}{\prod_{k=1}^{i}(p_ir+1)}, \qquad i = 1, \ldots, M. \end{aligned} \quad (41)$$

Therefore, in our model the natural boundary conditions for the put option price are

$$\begin{cases} P(S,T_i,K) = 0, & K \to 0, \\ P(S,T_i,K) = A(T_i)K - B(T_i)S \approx A(T_i)K, & K \to \infty, \end{cases} \quad (42)$$

A similar equation can be obtained for the call option prices; the equation reads

$$\left[\frac{1}{2}\sigma^2(K)K^2\nabla_K^2 + (r-q)K\nabla_K - \left(q + \frac{1}{X(T_i) - X(T_{i-1})}\right)\right] C(S,T_i,K) = -\frac{C(S,T_{i-1},K)}{X(T_i) - X(T_{i-1})} \quad (43)$$

subject to the boundary conditions

$$\begin{cases} C(S,T_i,K) = B(T_i)S, & K \to 0, \\ C(S,T_i,K) = 0, & K \to \infty. \end{cases} \quad (44)$$

PIECEWISE MODELS OF LOCAL VARIANCE/VOLATILITY

To calibrate the local volatility surface by solving Equation 37 we need to make further assumptions about the shape of the local volatility surface. Recall, we assume this surface to be piecewise constant in time. In the strike space Carr and Nadtochiy (2017) considered it to be a piecewise constant, while in Carr and Itkin (2018) a piecewise linear local variance in the strike space was considered. As shown in Carr and Itkin (2018), in those cases Equation 37 can be solved in closed form.

In this article we want to extend a class of local volatility models that allow a closed form solution. To proceed, we start by doing a change of the dependent variable from $P(S, T_j, K)$ to

$$V(S,T_j,K) = P(S,T_j,K) - [A(T_j)K - B(T_j)S]^+, \quad (45)$$

where V is known as a *covered* put. This definition of V allows rewriting Equation 37 in a more elegant form:

$$\begin{gathered} -v_j(x)x^2V_{x,x}(x) + b_{1,j}xV_x(x) + b_{0,j}V(x) = c_j(x), \\ b_{1,j} = p_j(r-q), \quad b_{0,j} = p_jq + 1, \\ c_j(x) = V(S,T_{j-1},x), \quad v_j(x) = p_j\sigma^2(x)/2, \end{gathered} \quad (46)$$

where $V(x) = V(S, T_j, x)$, and $x = K/S$ is the inverse moneyness.

Accordingly, based on the definition of $V(x)$ and Equation 42, the boundary conditions to Equation 46 become homogeneous:

$$\begin{cases} V(x) = 0, & x \to 0, \\ V(x) = 0, & x \to \infty. \end{cases} \quad (47)$$

In the next sections we consider several popular approximations of the local volatility surface in the strike space. Each approximation assumes some functional form of the local volatility curve in the strike space, which is a strip of the volatility surface given time to maturity T. Thus, parameters of these approximations change with time. Also, further on for simplicity we assume that $r > q > 0$, but this assumption could be easily relaxed.

Local Variance Piecewise Linear in Log-Strike Space

Suppose that for each maturity T_j, $j \in [1, M]$ the market quotes are provided for a set of strikes K_i, $i = 1, \ldots, n_j$ where these strikes are assumed to be sorted in increasing order. Then the corresponding continuous piecewise linear local variance function $\sigma_j^2(\chi)$ at the interval $[\chi_i, \chi_{i+1}]$, $\chi = \log K_i/S$, reads

$$v_{j,i}(\chi) = v_{j,i}^0 + v_{j,i}^1\chi. \quad (48)$$

Here we use the super-index 0 to denote a level v^0 and the super-index 1 to denote a slope v^1. Subindex $i = 0$ in $v_{j,0}^0, v_{j,0}^1$ corresponds to the interval $(0, \chi_1]$. Since $v_j(\chi)$ is a continuous function in χ, we have

$$v_{j,i}^0 + v_{j,i}^1\chi_{i+1} = v_{j,i+1}^0 + v_{j,i+1}^1\chi_{i+1}, \qquad i = 0, \ldots, n_j - 1. \quad (49)$$

This result means that the first derivative of $v_j(\chi)$ experiences a jump at points χ_i, $i \in [1, n_j]$. As we assumed that $v(\chi, T)$ is a piecewise constant function of time, and do not depend on T at the intervals $[T_j, T_{j+1})$, $j \in [0, M-1]$ and jump to the new values at the points T_j, $j \in [1, M]$.

A simple analysis shows that under this assumption, by making a change of variables $x \to \chi$, Equation 46 could be transformed to

$$-v(\chi)V_{\chi,\chi}(\chi) + (b_1 + v(\chi))V_\chi(\chi) + b_0V(\chi) = c(\chi), \quad (50)$$

where for simplicity of notation we dropped index j.

This equation is the same type as that considered in Itkin and Lipton (2018, section 2), and its solution could also be expressed in terms of confluent hypergeometric functions (see Polyanin and Zaitsev 2003):

$$\begin{gathered} V(\chi) = C_1\gamma_1(\chi) + C_2\gamma_2(\chi) + I_{12}(\chi) \\ I_{12}(\chi) = \gamma_2(\chi)\int \frac{\gamma_1(\chi)c(\chi)}{(b_2 + a_2\chi)W}d\chi - \gamma_1(\chi)\int \frac{\gamma_2c(\chi)}{(b_2 + a_2\chi)W}d\chi, \end{gathered} \quad (51)$$

where $W = \gamma_1(\gamma_2)_\chi - \gamma_2(\gamma_1)_\chi$ is the so-called Wronskian of the fundamental solutions γ_1, γ_2, and C_1, C_2 are some constants. Thus, the problem is reduced to finding suitable fundamental solutions of the homogeneous version

of Equation 50. Based on Polyanin and Zaitsev (2003), if $a_2 \neq 0$ and $b_0 \neq 0$, the general solution reads

$$V(\chi) = (a_2 z)^{\beta_1 - 1} \mathcal{J}(\alpha_1, \beta_1, z),$$
$$z = \chi + \frac{b_2}{a_2}, \quad \alpha_1 = 1 + \frac{b_0 + b_1}{a_2}, \quad \beta_1 = 2 + \frac{b_1}{a_2}. \quad (52)$$

Here $\mathcal{J}(a, b, z)$ is an arbitrary solution of the degenerate hypergeometric equation, that is, Kummer's function (Abramowitz and Stegun 1964). Two types of Kummer's functions are known, namely $M(a, b, z)$ and $U(a, b, z)$, which are Kummer's functions of the first and second kind.[4]

Accordingly, the approach of Itkin and Lipton (2018) can be directly applied to obtain a closed form solution of Equation 51. In particular, in the vicinity of the origin, the numerically satisfactory pair is (Olver 1997)

$$\gamma_1(\chi) = (a_2 z)^{\beta_1 - 1} M(\alpha_1, \beta_1, z),$$
$$\gamma_2(\chi) = (a_2)^{\beta_1 - 1} M(\alpha_1 - \beta_1 + 1, 2 - \beta_1, z).$$
$$W = a_2^{2\beta_1 - 2} e^z z^{\beta_1 - 2} \sin(\pi\beta_1)/\pi. \quad (53)$$

However, in the vicinity of infinity the numerically satisfactory pair is (Olver 1997)

$$\gamma_1(\chi) = (a_2 z)^{\beta - 1} U(\alpha_1, \beta_1, z),$$
$$\gamma_2(\chi) = e^z (a_2 z)^{\beta - 1} U(\beta_1 - \alpha_1, \beta_1, -z).$$
$$W = (-1)^{\alpha_1 - \beta_1} a_2^{2\beta_1 - 2} e^z z^{\beta_1 - 2}. \quad (54)$$

Local Variance Piecewise Linear in Strike Space

Another tractable model is one in which the local variance is piecewise linear in the strike space. In particular, this is the model we used in Carr and Itkin (2018).

Similar to the previous section, the corresponding continuous piecewise linear local variance function $\nu_j(x)$ at the interval $[x_i, x_{i+1}]$ reads

$$\nu_{j,i}(x) = \nu^0_{j,i} + \nu^1_{j,i} x, \quad (55)$$

where, however, it is now a function of x rather than χ. Since $\nu_j(x)$ is a continuous function in x, we have

$$\nu^0_{j,i} + \nu^1_{j,i} x_{i+1} = \nu^0_{j,i+1} + \nu^1_{j,i+1} x_{i+1}, \quad i = 0, \ldots, n_j - 1. \quad (56)$$

This result means that the first derivative of $\nu_j(x)$ experiences a jump at points x_i, $i \in Z[1, n_j]$. As we assumed that $\nu(x, T)$ is a piecewise constant function of time, $\nu^0_{j,i}$, $\nu^1_{j,i}$ do not depend on T at the intervals $[T_j, T_{j+1})$, $j \in [0, M-1]$, and jump to the new values at the points T_j, $j \in [1, M]$.

Equation 46 can be solved by induction. One starts with $T_0 = 0$ and at each time interval $[T_{j-1}, T_j]$, $j \in [1, M]$ solves the problem in Equation 46 for $V(x)$, and then obtains $P(S, T_j, x)$ from Equation 45. Accordingly, the solution of Equation 46 can be constructed separately for each interval $[x_{i-1}, x_i]$.

Substituting the representation in Equation 55 into Equation 46, for the ith spatial interval, we obtain

$$-(b_2 + a_2 x) x^2 V_{x,x}(x) + b_1 x V_x(x) + b_{0,j} V(x) = c(x),$$
$$b_2 = \nu^0_{j,i}, \quad a_2 = \nu^1_{j,i}. \quad (57)$$

Again, Equation 57 is an *inhomogeneous* ODE, and its solution can be represented in the form of Equation 51 with

$$I_{12}(x) = -\gamma_2(x) \int \frac{\gamma_1(x) c(x)}{(b_2 + a_2 x) x^2 W(x)} dx$$
$$+ \gamma_1(x) \int \frac{\gamma_2(x) c(x)}{(b_2 + a_2 x) x^2 W(x)} dx \equiv J_1 + J_2. \quad (58)$$

The corresponding homogeneous equation can be solved as follows. First, if $b_2 \neq 0$, we make a change in the independent variable $x \mapsto z = -a_2 x / b_2$. As a result the homogeneous Equation 57 takes the form

$$b_2 (z - 1) z V_{z,z}(z) + b_1 z V_z(z) + b_0 V(z) = 0. \quad (59)$$

Then we change the dependent variable $V(z) \mapsto z^m G(z)$ with m being some constant for the given time slice. That change leads to the equation

$$z^m [\gamma + b_2 (m-1) m z] G(z) + z^{m+1} [b_1 + 2 b_2 m (z-1)]$$
$$G'(z) + b_2 (z-1) z^{m+2} G''(z) = 0,$$
$$\gamma = b_0 + m(b_2 + b_1 - b_2 m). \quad (60)$$

Next we solve for m, which makes γ vanish, to obtain

[4] Because of the linearity of the degenerate hypergeometric equation, any linear combination of Kummer's functions also solves this equation.

$$m^{\pm} = \frac{b_2 + b_1 \pm \sqrt{4b_2 b_0 + (b_2 + b_1)^2}}{2b_2}. \tag{61}$$

Notably, if the determinant D in this expression is negative, both m^+ and m^- become complex. However, this is not a problem for the solution as coefficients C_1, C_2 in Equation 51 could be complex as well, and such that the put price is real.

Substituting this into Equation 60 and rearranging, we obtain

$$-m(m-1)G(z) + \left(2m - \frac{b_1}{b_2} - 2mz\right)G'(z) + z(1-z)G''(z) = 0, \quad m \in [m^+, m^-], \tag{62}$$

which is a hypergeometric equation. As m can take two values, we need to choose the right one such that the final solution would obey the boundary conditions.

Combining all the above steps, the solution of Equation 59 could be written as

$$\begin{aligned} &y_1(x) = z^m[{}_2F_1(m-1, m, c; z)], \\ &y_2(x) = z^m[z^{1-c}{}_2F_1(m-c, m+1-c, 2-c; z)], \\ &m = m^+, \quad c = 2m - \frac{b_1}{b_2}, \quad z = -\frac{a_2}{b_2}x. \end{aligned} \tag{63}$$

Here ${}_2F_1(a, b, c; z)$ is the ordinary hypergeometric function (Olver 1997). It has regular singularities at $z = 0$, $1, \infty$. In regard to the solution in Equation 52, these singularities correspond to $K = 0$, $v = 0$, and $K \to \infty$. We will show below that at $K \to \infty$, the coefficient a_2 for this interval is usually positive, so the variance is positive. However, the sign of b_2 could be both plus and minus. Therefore, if $b_2 > 0$ at this interval, we have $x \to \infty$, $z \to -\infty$. If $b_2 < 0$ at this interval, we have $x \to \infty$, $z \to \infty$.

When neither c, $c - a - b$, nor $a - b$ is an integer, we have a pair of fundamental solutions, $f_1(x), f_2(x)$, that in Equation 52 are represented by expressions in square brackets. It is known that this pair is numerically satisfactory (Olver 1997) aside from singularities at $z = 1$ and $z \to \infty$. The Wronskian of these fundamental solutions $W(f_1(x), f_2(x))$ is

$$W(f_1(x), f_2(x)) = (1-c)z^{-c}(1-z)^{c-2m}, \quad z = -a_2 x / b_2.$$

Accordingly,

$$W(\gamma_1(x), \gamma_2(x)) = -\frac{a_2(1-c)}{b_2} z^{2m-c}(1-z)^{c-2m}, \quad z = -a_2 x / b_2. \tag{64}$$

In the vicinity of the **singularity at $z = 1$**, this pair, however, is not numerically satisfactory. Then we have to use another solution of Equation 62, which is (Olver 1997)

$$\begin{aligned} &\gamma_1(x) = z^m[{}_2F_1(m-1, m, 2m-c; 1-z)], \\ &\gamma_2(x) = z^m[(1-z)^{c-2m+1}{}_2F_1(c-m+1, c-m, c-2m+2; 1-z)], \\ &W(\gamma_1(x), \gamma_2(x)) \\ &\quad = -\frac{a_2(2m-1-c)}{b_2}(1-z)^{c-2m} z^{2m-c}, \quad z = -a_2 x / b_2. \end{aligned} \tag{65}$$

The numerically satisfactory fundamental solutions in the vicinity of the **singularity at $z = \infty$** are described in Appendix A.

However, we cannot use this solution at $z \to \infty$ as well as using the solution in Equation 63 at $z \to 0$. This is caused by the Roger Lee's moment matching formula (Lee 2004), which states that in the wings the implied variance surface should be at most linear in the normalized strike (or log-strike). It is also shown in De Marco, Friz, and Gerhold (2013) and Gerhold and Friz (2015) that the asymptotic behavior of the local variance is linear in the log-strike at both $K \to \infty$ and $K \to 0$. While the result for $K \to 0$ is shown to be true at least for the Heston and Stein–Stein models, the result for $K \to \infty$ directly follows from Lee's moment formula for the implied variance v_I and the representation of σ^2 via the total implied variance $w = v_I T$ (Lipton 2001 and Gatheral 2006)

$$w_L \equiv \sigma^2(T, K)T = \frac{T\partial_T w}{\left(1 - \frac{X\partial_X w}{2w}\right)^2 - \frac{(\partial_X w)^2}{4}\left(\frac{1}{w} + \frac{1}{4}\right) + \frac{\partial_X^2 w}{2}}, \tag{66}$$

where $w = w(X, T)$ and $X = \log K/F$, and $F = Se^{(r-q)T}$ is the stock forward price.

Thus, the considered model where the local variance is linear in strike is not applicable at the first $0 \le x \le x_1$ and the last $x_{nj} < x < \infty$ strike intervals for every

smile $T = T_j$ as it violates Lee's formula. Therefore, at these two intervals we use the model discussed previously in this section in which the local variance is linear in the log-strike.

It is interesting to note that in Itkin and Lipton (2018), Carr and Itkin (2018), and previously in this section, the closed form solution was obtained in terms of Kummer's functions. Here the solution is expressed via hypergeometric functions ${}_2F_1(a, b, c; x)$.

As two solutions $\gamma_1(x)$ and $\gamma_2(x)$ are independent, Equation 51 is a general solution of Equation 57. Two constants C_1, C_2 should be determined on the basis of the boundary conditions for the function $\gamma(x)$.

The boundary conditions for the ODE Equation 57 in the x space at zero and infinity are given in Equation 47, that is, they are homogeneous. On the basis of the usual shape of the local variance curve and its positivity, for $x \to 0$, we expect that $\nu^1_{j,i} < 0$. Similarly, for $x \to \infty$ we expect that $\nu^1_{j,i} > 0$. In between these two limits the local variance curve for a given maturity T_j is assumed to be continuous, but the slope of the curve could be both positive and negative (see, e.g., Itkin 2015 and references therein).

Local Volatility Piecewise Linear in Strike Space

Another popular model is one in which the local volatility is assumed to be piecewise linear in the strike space. This model previously was frequently considered in the literature, for example, Hull and White (2015) and Kienitz and Caspers (2017). Below we show that with this assumption our model remains tractable, and a closed form solution can be obtained by using the same approach as elaborated on in Itkin and Lipton (2018) and Carr and Itkin (2018).

Accordingly, the corresponding continuous piecewise linear local volatility function $\sigma_j(x)$ on the interval $[x_i, x_{i+1}]$ reads

$$\sigma_{j,i}(x) = \sigma^0_{j,i} + \sigma^1_{j,i} x. \tag{67}$$

Since $\sigma_j(x)$ is a continuous function in x, we have

$$\sigma^0_{j,i} + \sigma^1_{j,i} x_{i+1} = \sigma^0_{j,i+1} + \sigma^1_{j,i+1} x_{i+1}, \quad i = 0, \ldots, n_j - 1. \tag{68}$$

Again, this means that the first derivative of $\sigma_j(x)$ experiences a jump at points x_i, $i \in [1, n_j]$. As $\sigma(x, T)$ is a piecewise constant function of time, $\sigma^0_{j,i}, \sigma^1_{j,i}$ do not depend on T at the intervals $[T_j, T_{j+1})$, $j \in 0, M-1]$ and jump to the new values at the points T_j, $j \in [1, M]$.

Substituting representation in Equation 67 into Equation 46, for the ith spatial interval, we obtain

$$-(b_2 + a_2 x)^2 x^2 V_{x,x}(x) + b_1 x V_x(x) + b_{0,j} V(x) = c(x),$$
$$b_2 = \sigma^0_{j,i}, \quad a_2 = \sigma^1_{j,i}. \tag{69}$$

Again, Equation 69 is an *inhomogeneous* ODE, and its solution can be represented in the form of Equation 51 with

$$I_{12}(x) = -\gamma_2(x) \int \frac{\gamma_1(x) c(x)}{(b_2 + a_2 x)^2 x^2 W(x)} dx + \gamma_1(x) \int \frac{\gamma_2(x) c(x)}{(b_2 + a_2 x)^2 x^2 W(x)} dx \equiv L_1 + L_2.$$

The corresponding homogeneous equation can be solved as follows. First, if $b_2 \neq 0$, $b_2 + a_2 x \neq 0$, we make a change of the independent variable $x \mapsto z = a_2 b_1 x / [b_2^2 (b_2 + a_2 x)]$. As a result the homogeneous Equation 69 takes the form

$$b_2 z^2 (-b_1 + b_2^2 z) V_{z,z}(z) + z[2b_2^4 z + (b_1 - b_2^2 z)^2] V_z(z) + b_0 (b_1 - b_2^2 z) V(z) = 0.$$

Next, we make a change in the dependent variable

$$V(z) \mapsto z^{k_1} \left(\frac{z}{b_2^2 z + b_1} \right)^{k_2} G(z)$$

with k_1, k_2 being some constants for the given time slice. This change leads to the equation

$$\begin{aligned}
0 &= -b_2^2 z (b_1 - b_2^2 z)^2 G''(z) + f_1(z) G'(z) + f_0(z) G(z), \\
f_1(z) &= z(b_1 - b_2^2 z)[b_2^4 z(2k_1 + z + 2) - 2b_2^2 b_1 (k_1 + k_2 + z) + b_1^2], \\
f_0(z) &= q_0 + q_1 z + q_2 z^2 - b_2^6 k_1 z^3, \\
q_2 &= b_2^4 [b_0 - b_2^2 k_1 (k_1 + 1) + b_1 (3k_1 + k_2)], \\
q_1 &= b_2^2 b_1 [2b_2^2 k_1 (k_1 + k_2) - 2b_0 - b_1 (3k_1 + 2k_2)], \\
q_0 &= b_1^2 [b_0 - (k_1 + k_2)(b_2^2 (k_1 + k_2 - 1) - b_1)].
\end{aligned} \tag{70}$$

We now request that $f_0(z)$ be proportional to $z(b_1 - b_2^2 z)^2$ with some constant multiplier q, that is,

$$f_0(z) = qz(b_1 - b_2^2 z)^2.$$

Solving this equation term by term in powers of z, we obtain

$$k_1 = -\frac{q}{b_2^2}, \quad k_2 = \frac{q(b_1+q) - b_2^2(b_0+q)}{b_2^2 b_1},$$
$$q = \frac{1}{2}\left(b_2^2 - b_1 \pm \sqrt{b_2^4 + 2b_2^2(2b_0+b_1) + b_1^2}\right).$$

Accordingly, substituting these definitions into Equation 70, we find

$$0 = zG''(z) + (b+z)G'(z) - aG(z),$$
$$b = 2 - \frac{b_1 + 2q}{b_2^2}, \quad a = \frac{q}{b_2^2}.$$

This is a sort of Kummer equation that has two independent solutions (Polyanin and Zaitsev 2003):

$$G(z) = e^{-z}U(a+b,b,z), \quad G(z) = e^{-z}M(a+b,b,z). \quad (71)$$

Accordingly, as q can take two values corresponding to the plus and minus sign, we have four fundamental solutions of the original equation, Equation 70.

Similar to in the previous section, we cannot use these solutions at the first $0 \le x \le x_1$ and the last $x_{nj} < x < \infty$ strike intervals for every smile $T = T_j$ as that violates Lee's formula. Therefore, at these two intervals we use the model discussed previously in which the local variance is linear in the log-strike. Accordingly, the local volatility is a square root of the local variance.

COMPUTATION OF SOURCE TERM

Computation of the source term pI_{12} in Equation 51 could be achieved in several ways. The most straightforward one is to use numerical integration since the put price $P(x, T_{i-1})$ as a function of x is already known when we solve Equation 51 for $T = T_i$. We underline that this is not the case in Itkin and Lipton (2018) because there the function $P(x, T_{i-1})$ is obtained by using an inverse Laplace transform and as such is known only for a discrete set of strikes at the previous time level. Therefore, some kind of interpolation is necessary to find the local variance at all strikes when carrying out integration. Moreover, this interpolation must preserve no-arbitrage (see Itkin and Lipton 2018).

However, using no-arbitrage interpolation provides another advantage as it makes it possible to compute the source term integrals in closed form if the interpolating function is wisely chosen. Here we want to exploit the same idea, thus significantly improving the computational performance of our model as compared with the numerical integration.

Below as an example consider the case of the local variance piecewise linear in the strike space. Then based on solutions found previously in this section, in Equation 63 we have

$$J_1(x) = -\gamma_2(x)\int \frac{\gamma_1(x)c(x)}{(b_2 + a_2 x)x^2 W(x)}dx$$
$$= -\gamma_2(x)\frac{a_2^2}{b_2^3}\int \frac{\gamma_1(z)c(z)}{(1-z)z^2 W(z)}dz,$$
$$\gamma_1(z) = z^m\, {}_2F_1(m-1,m,c;z),$$
$$c(z) = V(S,T_{j-1},z), \quad z = -a_2 x/b_2, \quad (72)$$

where $W(z)$ is defined in Equation 64.

Following the idea of Itkin and Lipton (2018), in Carr and Itkin (2018) we introduced a nonlinear interpolation:

$$P(x) = \gamma_0 + \gamma_2 x^2, \quad x_1 \le x \le x_3,$$
$$\gamma_0 = \frac{P(x_3)x_1^2 - P(x_1)x_3^2}{x_1^2 - x_3^2},$$
$$\gamma_2 = \frac{P(x_1) - P(x_3)}{x_1^2 - x_3^2}. \quad (73)$$

Then Proposition 6.1 in Carr and Itkin (2018) proves that this interpolation scheme is arbitrage free.

It is worth emphasizing that the proposed interpolation does not affect the solution values (quotes) at given market strikes since the piecewise interpolator is constructed to exactly match those values. So the interpolation affects only the put values that are not known, that is, those with strikes that lie in between the given market strikes. Therefore, if these strikes are not used, that is, in trading or hedging, the influence of the interpolation is not observable at all. If, however, they are used for some

purpose, the difference with the exact solution is small (within the error of interpolation), yet the approximate solution for these strikes preserves no-arbitrage.

Recall that we introduced $V(x)$ using Equation 45. Accordingly, the term $c(z)$ in Equation 72 takes the form (see Appendix D and Equation D3)

$$c(z) = V(S, T_{j-1}, z) = \overline{\gamma}_0 + \gamma_1 z + \overline{\gamma}_2 z^2. \tag{74}$$

It becomes apparent that now the integral in Equation 72 can be computed in closed form. Indeed

$$\begin{aligned}
&\int \frac{\gamma_1(z)c(z)}{(1-z)z^2W(z)}dz = I_0 + I_1 + I_2,\\
&I_0 = \gamma_0 \int \frac{\gamma_1(z)}{(1-z)z^2W(z)}dz\\
&\quad = \overline{\gamma}_0 A(z)\frac{1}{\Gamma(c)(c-m-1)}\,{}_2F_1(c-m-1, c-m+1, c, z),\\
&I_1 = \gamma_1 \int \frac{z\gamma_1(z)}{(1-z)z^2W(z)}dz\\
&\quad = \gamma_1 z A_{(z)}\frac{1}{\Gamma(c)(c-m)}\,{}_2F_1(c-m, c-m, c, z)\\
&I_2 = \overline{\gamma}_2 \int \frac{z^2\gamma_1(z)}{(1-z)z^2W(z)}dz\\
&\quad = \overline{\gamma}_2 A(z)z^2\frac{1}{(c-m+1)\Gamma(c)}\,{}_3\\
&\qquad F_2[c-m, c-m+1, c-m+1, c, 2+c-m; z],\\
&A(z) = \frac{b_2}{a_2}\Gamma(c-1)z^{c-m-1},
\end{aligned} \tag{75}$$

where ${}_3F_2\left[\begin{matrix} a_1, a_2, a_3 \\ b_1, b_2 \end{matrix}; z\right]$ is a generalized hypergeometric function (Askey and Daalhuis 2010).

The second integral in the definition of J_{20}

$$\begin{aligned}
J_2(x) &= \gamma_1(x)\int \frac{\gamma_2(x)c(x)}{(b_2 + a_2 x)x^2W(x)}dx\\
&= \gamma_1(x)\frac{a_2^2}{b_2^3}\int \frac{\gamma_2(z)c(z)}{(1-z)z^2W(z)}dz,\\
\gamma_2(z) &= z^{m+1-c}\,{}_2F_1(m-c, m+1-c, 2-c; z),
\end{aligned} \tag{76}$$

could be computed in a similar way. The result reads

$$\begin{aligned}
&\int \frac{\gamma_2(z)c(z)}{(1-z)z^2W(z)}dz = \mathcal{I}_0 + \mathcal{I}_1 + \mathcal{I}_2,\\
&\mathcal{I}_0 = \gamma_0 \int \frac{\gamma_2(z)}{(1-z)z^2W(z)}dz\\
&\quad = \overline{\gamma}_0 A(z)\frac{1}{m}\,{}_2F_1(2-m, -m, 2-c, z),\\
&\mathcal{I}_1 = \gamma_1 \int \frac{z\gamma_2(z)}{(1-z)z^2W(z)}dz\\
&\quad = \gamma_1 A(z)z\frac{1}{(m-1)}\,{}_2F_1(1-m, 1-m, 2-c, z),\\
&\mathcal{I}_2 = \overline{\gamma}_2 \int \frac{z^2\gamma_2(z)}{(1-z)z^2W(z)}dz\\
&\quad = \overline{\gamma}_2 A(z)z^2\frac{1}{(m-2)}\,{}_3\\
&\qquad F_2[1-m, 2-m, 2-m, 2-c, 3-m; z],\\
&A(z) = \frac{b_2}{a_2}\frac{\Gamma(1-c)}{\Gamma(2-c)}z^{-m}.
\end{aligned} \tag{77}$$

Two special cases are the first $0 \le x \le x_1$ and the last $x_{n_j} < x < \infty$ intervals, for which the solution is given by Equations 53 and 54.

Last Interval $x_{n_j} \le x < \infty$

Since the right edge of the last interval lies at infinity, the interpolation scheme in Equation 73 should be slightly modified. This modification could be done twofold. The first option is to move the boundary from infinity to any very large but finite positive strike. Then the scheme in Equation 73 could be used with no difficulty. But in our case it becomes apparent that we are not able to compute these integrals in closed form. Therefore, we use another approach that consists in replacing the quadratic form in Equation 73 with another nonlinear interpolation

$$c(\chi) = V(\chi, T_{j-1}, S) = \gamma_\infty z^{-\nu}, \quad z = \chi + \frac{b_2}{a_2}, \tag{78}$$

where $\gamma_\infty > 0$, $\nu > 0$ are some constants to be determined. Obviously, at $\chi \to \infty$ this interpolation preserves the correct boundary value of V as in Equation 47, that is, $V(\chi)$ vanishes in this limit. The derivation of the appropriate

values of γ_∞, ν and a proof that the proposed interpolation preserves no-arbitrage are given in Appendix B.

Recall that at this interval we assume the local variance to be linear in the log-strike χ. Therefore, the numerically stable pair of solutions of Equation 51 is given in Equation 54. Then the integral in Equation 51 can be computed in closed form. In doing so we use the following notation from Ng and Geller (1970):

$$\int e^{-\alpha z} z^{\upsilon} U(a,b,z)dz = U_{\upsilon}(\alpha;a,b,z),$$
$$\int e^{-\alpha z} z^{\upsilon} M(a,b,z)dz = M_{\upsilon}(\alpha;a,b,z).$$

Then

$$I_{12}(\chi) = \gamma_2(\chi)\int \frac{\gamma_1(\chi)c(\chi)}{(b_2+a_2\chi)W}d\chi - \gamma_1(\chi)\int \frac{\gamma_2(\chi)c(\chi)}{(b_2+a_2\chi)W}d\chi,$$
$$\int \frac{\gamma_1(\chi)c(\chi)}{(b_2+a_2\chi)W}d\chi = \xi_\infty \int e^{-z} z^{-\nu} U(\alpha_1,\beta_1,z)dz$$
$$= \xi_\infty U_{-\nu}(-1;\alpha_1,\beta_1,z),$$
$$\int \frac{\gamma_2(\chi)c(\chi)}{(b_2+a_2\chi)W}d\chi = \xi_\infty \int z^{-\upsilon} U(\beta_1-\alpha_1,\beta_1,-z)dz$$
$$= (-1)^{-\upsilon}\xi_\infty U_{-\upsilon}(0;\beta_1-\alpha_1,\beta_1,-z),$$
$$\xi_\infty = (-1)^{\beta_1-\alpha_1}\gamma_\infty a_2^{2-\beta_1}. \qquad (79)$$

As per Ng and Geller (1970),

$$M_\nu(-1;a,b,z) = e^{i\pi(\nu+1)}M_\nu(0;b-a,b,-z),$$
$$M_\nu(0;a,b,z) = \frac{z^{\nu+1}}{\nu+1}\,{}_2F_2\left[\begin{matrix}\nu_1+1, a\\ \nu+2, b\end{matrix};\ z\right]$$
$$b \neq 0,-1,-2,\ldots, \quad \nu \neq -1,-2,\ldots,$$
$$M_{-1}(0;a,b,z) = \frac{a}{b}z\,{}_3F_3\left[\begin{matrix}a+1, 1, 1\\ b+1, 2, 3\end{matrix};\ z\right] + \log(z),$$
$$U_\nu(\alpha;a,b,z) = \frac{\pi}{\sin(\pi b)}\left[\begin{matrix}\dfrac{M_\nu(\alpha;a,b,z)}{\Gamma(1+a-b)\Gamma(b)}\\ -\dfrac{M_{\nu+1-b}(\alpha;1+a-b,2-b,z)}{\Gamma(a)\Gamma(2-b)}\end{matrix}\right]. \qquad (80)$$

Therefore, all necessary integrals could be expressed in terms of generalized hypergeometric functions. Alternatively, these integrals could be represented as

$$U_{-\nu}(-1;\alpha_1,\beta_1,z) = G^{2,1}_{2,3}\left(\begin{matrix}1, 2+\alpha_1-\beta_1-\nu\\ 1-\nu, 2-\beta_1-\nu, 0\end{matrix}\ \middle|\ z\right),$$
$$U_{-\nu}(0;\alpha_1,\beta_1,-z) = \frac{z^{1-\nu}}{\Gamma(1-\alpha_1)\Gamma(\beta_1-\alpha_1)}$$
$$G^{2,2}_{2,3}\left(\begin{matrix}\nu, 1+\alpha_1-\beta_1\\ 0, 1-\beta_1, \nu-1\end{matrix}\ \middle|\ -z\right), \qquad (81)$$

where $G^{m,n}_{p,q}\left(\begin{matrix}a_1,\ldots,a_p\\ b_1,\ldots,b_q\end{matrix}\ \middle|\ z\right)$ is the Meijer G-function (see Olver 1997).

It is not difficult to verify that at $K \to \infty$, and so $z \to \infty$, the integral $I_{12}(\chi)$ vanishes.

First Interval $0 \le x \le x_1$

Recall that at the first interval we assume the local variance to be linear in the log-strike χ. Since at $K \to 0$ we have $\chi \to -\infty$, the numerically stable pair of solutions of Equation 51 is still given by Equation 54.

However, at this interval we need another interpolation scheme because the previously described schemes do not give rise to tractable integrals. However, this could be achieved by using, for example, the following nonlinear interpolation:

$$c(\chi) = V(\chi, T_{j-1}, S) = \omega_0 e^z/z, \quad z = \chi + \frac{b_2}{a_2}, \qquad (82)$$

where $\omega_0 < 0$ is a constant to be determined. Obviously, at $K \to 0$, and so $z \to -\infty$, this interpolation preserves the correct boundary value of V as in Equation 47, that is, $V(\chi)$ vanishes in this limit. The derivation of the appropriate value of ω_0 and a proof that the proposed interpolation preserves no-arbitrage are given in Appendix C.

Now the integral in Equation 51 can be computed in closed form:

$$
\begin{aligned}
I_{12}(\chi) &= \gamma_2(\chi)\int \frac{\gamma_1(\chi)c(\chi)}{(b_2+a_2\chi)W}d\chi - \gamma_1(\chi)\int \frac{\gamma_2(\chi)c(\chi)}{(b_2+a_2\chi)W}d\chi,\\
\int \frac{\gamma_1(\chi)c(\chi)}{(b_2+a_2\chi)W}d\chi &= \xi_0\int z^{-1}U(\alpha_1,\beta_1,z)dz\\
&= \xi_0 U_{-1}(0;\alpha_1,\beta_1,z),\\
\int \frac{\gamma_2(\chi)c(\chi)}{(b_2+a_2\chi)W}d\chi &= \xi_0\int e^z z^{-1}U(\beta_1-\alpha_1,\beta_1,-z)dz\\
&= -\xi_0 U_{-1}(-1;\beta_1-\alpha_1,\beta_1,z),\\
\xi_0 &= (-1)^{\beta_1-\alpha_1}\omega_0 a_2^{-\beta_1}.
\end{aligned}
\tag{83}
$$

Representation of functions $U_{-1}(-1;\beta_1-\alpha_1,\beta_1,z)$, $U_{-1}(0;\alpha_1,\beta_1,z)$ via the Meijer G-function is given in Equation 81. Again, it can be easily verified that at $K\to 0$, and so $z\to-\infty$, the integral $I_{12}(\chi)$ vanishes.

Special Case $z\approx 1$ or $|w/b_2|\ll 1$

The special case occurs when at the interval $[K_i,K_{i+1}]$ for some $i\in[1,n_j]$ coefficients, a_2, b_2 are such that either $|1-z_i|\ll 1$ or $|1-z_{i+1}|\ll 1$. Suppose, for example, that $z_{i+1}=1+\epsilon$ with $0<\epsilon\ll 1$. As shown in the next section, then we can introduce a ghost point K_* such that $z_*=1-\epsilon$. So at the interval $[K_*,K_{i+1}]$ we will use the numerically stable solution in Equation 65, while at the interval $[K_i,K_*]$ we will use the regular solution in Equation 63. Same construction could be provided if $z_i=1-\epsilon$.

At the interval $z\in[1-\epsilon,1+\epsilon]$ where the values of z are close to singularity of the hypergeometric function at $z=1$, there are two ways to construct the solution. First, one can build an asymptotic solution using w/b_2 as a small parameter because at $z\to 1$ we have $w/b_2=(b_2+a_2x)/b_2=1-z\to 0$. As shown in Carr and Itkin (2018), this can be done, for example, by using the method of boundary functions (Vasil'eva, Butuzov, and Kalachov 1995).

Alternatively, it follows from Equation 65 that $\gamma_1(z)\to 1$, $\gamma_2(z)\to 0$ at $z\to 1$. Therefore, these solutions have a regular behavior in the vicinity of $z=1$. So all we need to do is to propose a suitable no-arbitrage interpolation to make computation of the source term in Equation 58 tractable. This interpolation is constructed in Appendix D.

Thus, on the basis of Equation 72 and Equation 65, we need to compute two integrals:

$$
\begin{aligned}
\mathcal{J}_1(x) &= \int \frac{\gamma_1(z)c(z)}{(1-z)z^2W(z)}dz,\\
\mathcal{J}_2(x) &= \int \frac{\gamma_2(z)c(z)}{(1-z)z^2W(z)}dz,\\
\gamma_1(z) &= z^m\,{}_2F_1(m-1,m,2m-c;1-z),\\
c(z) &= V(z,T_{j-1},S),\\
\gamma_2(z) &= z^m(1-z)^{c-2m+1}\,{}_2\\
&\quad F_1(c-m+1,c-m,c-2m+2;1-z),\\
W(\gamma_1(z),\gamma_2(z)) &= \omega_1(1-z)^{c-2m}z^{2m-c},\\
\omega_1 &= -\frac{a_2(2m-1-c)}{b_2}.
\end{aligned}
\tag{84}
$$

The integral $\mathcal{J}_2(x)$ can be found in closed form, and the result reads

$$
\begin{aligned}
\mathcal{J}_2(x) &= \overline{\gamma}_0\mathcal{J}_{2,0}(x)+\gamma_1\mathcal{J}_{2,1}(x)+\overline{\gamma}_2\mathcal{J}_{2,1}(x),\\
\mathcal{J}_{2,0}(x) &= \frac{\pi}{\omega_1}\csc(\pi c)z^{-m}\Gamma(c-2m+2)\\
&\quad\left[\frac{z^{c-1}\,{}_2F_1(c-m-1,c-m+1;c;z)}{(c-m-1)\Gamma(c)\Gamma(1-m)\Gamma(2-m)}\right.\\
&\quad\left.+\frac{{}_2F_1(2-m,-m;2-c;z)}{m\Gamma(2-c)\Gamma(c-m)\Gamma(c-m+1)}\right],\\
\mathcal{J}_{2,1}(x) &= \frac{\pi}{(m-1)\omega_1}\csc(\pi c)z^{-m}\Gamma(c-2m+2)\\
&\quad\left[\left(\frac{z(c-m)\,{}_2F_1(1-m,1-m;2-c;z)}{\Gamma(2-c)\Gamma(c-m+1)^2}\right.\right.\\
&\quad\left.\left.-\frac{z^c\,{}_2F_1(c-m,c-m;c;z)}{(c-m)\Gamma(c)\Gamma(1-m)^2}\right)\right],\\
\mathcal{J}_{2,2}(x) &= \frac{\Gamma(c-2m+2)}{\omega_1\Gamma(1-m)\Gamma(2-m)\Gamma(c-m)\Gamma(c-m+1)}\\
&\quad G^{2,3}_{3,3}\left(\begin{matrix}1,1,2\\2-m,\,c-m+1,\,0\end{matrix}\,\middle|\,z\right).
\end{aligned}
\tag{85}
$$

The integral $\mathcal{J}_1(x)$ with the use of the no-arbitrage interpolation defined in Equation D3 reads

$$
\begin{aligned}
\mathcal{J}_1(x) &= \omega_1^{-1}\int(1-z)^{-c+2m-1}z^{c-m-2}\,{}_2F_1(m-1,m;2m-c;1-z)\\
&\quad(\overline{\gamma}_0+\gamma_1 z+\overline{\gamma}_2 z^2)dz.
\end{aligned}
$$

This integral can be computed as follows. Recall that $z \in [1-\epsilon, 1+\epsilon]$, $|\epsilon| \ll 1$. Therefore, the term z^k, $k \in \mathbb{R}$ can be expanded into a series around $z = 1$ to obtain

$$z^k = \sum_{i=0}^{\infty} (-1)^i \begin{pmatrix} k \\ i \end{pmatrix} (1-z)^i.$$

Then $\mathcal{J}_1(x)$ takes the form

$$\begin{aligned}
\mathcal{J}_1(x) = \omega_1^{-1} \Bigg\{ & \overline{\gamma}_0 \sum_{i=0}^{\infty} (-1)^i \begin{pmatrix} c-m-2 \\ i \end{pmatrix} \\
& \int (1-z)^{i-c+2m-1} {}_2F_1(m-1, 2m-c; 1-z)\, dz \\
& + \gamma_1 \sum_{i=0}^{\infty} (-1) i \begin{pmatrix} c-m-1 \\ i \end{pmatrix} \\
& \int (1-z)^{i-c+2m-1} {}_2F_1(m-1, m; 2m-c; 1-z)\, dz \\
& + \overline{\gamma}_2 \sum_{i=0}^{\infty} (-1)^i \begin{pmatrix} c-m \\ i \end{pmatrix} \\
& \int (1-z)^{i-c+2m-1} {}_2F_1(m-1, m; 2m-c; 1-z)\, dz \Bigg\} \\
= \omega_1^{-1} & \sum_{i=0}^{\infty} \upsilon_i \int (1-z)^{i-c+2m-1} {}_2F_1(m-1, m; 2m-c; 1-z)\, dz, \\
= \omega_1^{-1} & \sum_{i=0}^{\infty} \frac{\nu_i}{c-i-2m} (1-z)^{-c+i+2m} {}_3 \\
& F_2 \left[\begin{matrix} m-1, m, 2m-c+i \\ 2m-c, 2m+i-c+1 \end{matrix} ;\ 1-z \right],
\end{aligned}$$

$$\nu_i = (-1)^i \left[\begin{matrix} \overline{\gamma}_0 \begin{pmatrix} c-m-2 \\ i \end{pmatrix} \\ + \gamma_1 \begin{pmatrix} c-m-1 \\ i \end{pmatrix} + \overline{\gamma}_2 \begin{pmatrix} c-m \\ i \end{pmatrix} \end{matrix} \right]. \tag{86}$$

The exponent $-c + i + 2m = i + b_1/b_2$ is always positive if $b_2 > 0$ in the vicinity of $z = 1$. According to Appendix D, this condition on b_2 is valid if $1 - \epsilon \le z < 1$. Therefore, 2-3 terms in the expansion Equation 86 provide sufficient accuracy in the computation of the integral. However, this is also true when $1 + \epsilon > z > 1$ (and so b_2 is negative), which implies that the entire exponent is also negative, at least at low i. The reason is that the behavior of the product $(1-z)^{i+c+2m} {}_3F_2 \left[\begin{matrix} m-1, m, 2m-c+i \\ 2m-c, 2m+i-c+1 \end{matrix} ;\ 1-z \right]$ is regular even in this case.

Similarly, the source terms for other models of the local variance/volatility considered in previous sections could be computed in closed form. We leave this exercise to the reader.

SMILE CALIBRATION FOR A SINGLE TERM

The calibration problem for the local volatility model, as well as the construction of the solution for the entire smile, is described in Carr and Itkin (2018). Here, we follow the same approach and, therefore, provide just some short comments specific to the GLVG model. Again, as an example, consider the case in which the local variance is a piecewise linear function of strike. Calibration for the other cases considered in the section on piecewise models of local variance/volatility can be done similarly.

We need to solve a general calibration problem: given market quotes of call and/or put options corresponding to various strikes $\{K\} := K_j$, $j \in [1, N]$ and the same maturity T_i, find the local variance function $v(x)$ such that these quotes solve Equations 37 and 43.

Suppose that the put prices for $T = T_j$ are known for n_j ordered strikes. The location of those strikes on the x line is schematically depicted in Exhibit 1.

Recall that the general form of the solution is given in Equation 51, in which at every interval $x_{i-1} \le x \le x_i$ and $T = T_j$ can be represented as

$$V(x) = C_{j,i}^{(1)} \gamma_1(x) + C_{j,i}^{(2)} \gamma_2(x) + I_{12}(x). \tag{87}$$

Here for better readability we changed the notation of two integration constants that belong to the ith interval in x and jth maturity to $C_{j,i}^{(1)}, C_{j,i}^{(2)}$.

Similar to in Carr and Itkin (2018), we assume continuity of the options price and its first derivative at every node $i = 1, \ldots, n_j$. We also supplement this by two additional conditions: the first is given by Equation 49, and the other is that at every node the solution $P(S, T_j, K_i)$ must coincide with a given market quote for the pair (T_j, K_i). So together this provides four equations for the four unknown variables $v_{j,i}^0, v_{j,i}^1, C_{j,i}^{(1)}, C_{j,i}^{(2)}$:

EXHIBIT 1

Schematic Construction of Combined Solution in $x \in \mathbf{R}^+$

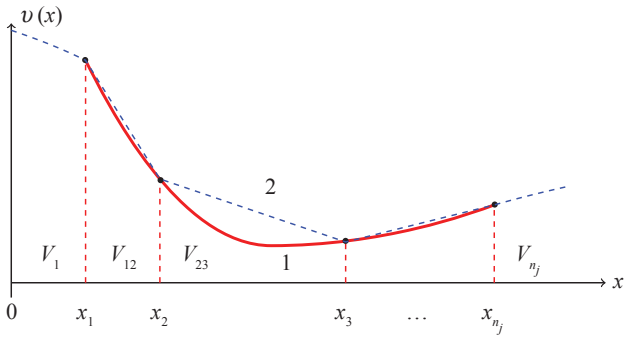

Notes: 1 (solid lines) = the real (unknown) local variance curve; 2 (dashed lines) = a piecewise linear solution. At $x > x_{n_j}$ and $x < x_1$ the dashed line is $b_2 + a_2 \log(x)$.

$$
\begin{aligned}
P_i(x)\big|_{x=x_i} &= P_{i+1}(x)\big|_{x=x_i}, \\
P_i(x)\big|_{x=x_i} &= P_{market}(x_i), \\
\frac{\partial P_{i+1}(x)}{\partial x}\bigg|_{x=x_i} &= \frac{\partial P_i(x)}{\partial x}\bigg|_{x=x_i}, \\
\nu^0_{j,i} + \nu^1_{j,i} x_i &= \nu^0_{j,i+1} + \nu^1_{j,i+1} x_i, \quad i = 1, \ldots, n_j.
\end{aligned} \tag{88}
$$

Equation 88 is a system of $4n_j$ nonlinear equations with respect to $4(n_j + 1)$ variables $\nu^0_{j,i}, \nu^1_{j,i}, C^{(1)}_{j,i}, C^{(2)}_{j,i}$. Therefore, we need four additional conditions to uniquely solve it.

For that purpose, observe that the constants $C^{(2)}_{j,1}$, $C^{(2)}_{j,n_j}$ could be determined according to the boundary conditions in Equation 47. Indeed, at $K \to 0$, the function $y_2(\chi)$ in Equation 54 vanishes (as $a_2 < 0$ at this interval), but not $y_1(x)$. Therefore, to obey the vanishing boundary condition in Equation 47, we must set $C^{(1)}_{j,1} = 0$. As that was already discussed, the source term in Equation 83 also vanishes in that limit. Therefore, the solution in Equation 54 with the source term in Equation 83 and $C^{(2)}_{j,1} = 0$ obeys the boundary condition at $z \to 0$.

At $K \to \infty$, according to the representation of the solution in Equation 54 with $a_2 > 0$ at this interval, similarly, we must set $C^{(2)}_{j,n_j} = 0$, as the solution $y_2(x)$ in Equation 54 diverges at $z \to \infty$.

The remaining two additional conditions could be set in many different ways. Here we rely on trader's intuition about the asymptotic behavior of the volatility surface at strikes close to zero and infinity. According to our construction, they are determined by $\nu^1_{j,0}$ and ν^1_{j,n_j}. Therefore, we assume these coefficients to be somehow known, that is, consider them as the given parameters of our model.

Overall, by solving the nonlinear system in Equation 88, we find the final solution of our problem. This can be done by using standard methods and, thus, no optimization procedure is necessary. However, a good initial guess still would be helpful for a better (and faster) convergence. The construction of such a guess is described in Carr and Itkin (2018). Also note that this system has a block-diagonal structure in which each block is a 2×2 matrix. Therefore, the problem can be easily solved with the linear complexity $O(n_j)$.

When computing the first derivatives, we take into account that derivatives of hypergeometric functions belong to the same class of functions, since (Abramowitz and Stegun 1964)

$$
\begin{aligned}
\frac{\partial}{\partial z}\, {}_2F_1(a,b,c,z) &= \frac{ab}{c}\, {}_2F_1(a+1,b+1,c+1,z), \\
\frac{\partial}{\partial z}\, {}_3F_2\left[\begin{matrix} a,b,c \\ d,e \end{matrix}; z\right] &= \frac{abe}{cd}\, {}_3F_2\left[\begin{matrix} a+1,b+1,c+1 \\ d+1,e+1 \end{matrix}; z\right].
\end{aligned}
$$

The same is true for the Meijer G-function. For instance,

$$
\begin{aligned}
&\frac{\partial}{\partial z} G^{2,2}_{2,3}\left(\begin{matrix} \nu, 1+\alpha_1-\beta_1 \\ 0, 1-\beta_1, \nu-1 \end{matrix}\bigg| -z\right) \\
&= \frac{\Gamma(1-\alpha_1)\Gamma(\beta_1-\alpha_1)}{z} U(\beta_1-\alpha_1, \beta_1, -z) \\
&\quad + (\nu-1)\, G^{2,2}_{2,3}\left(\begin{matrix} \nu, 1+\alpha_1-\beta_1 \\ 0, 1-\beta_1, \nu-1 \end{matrix}\bigg| -z\right).
\end{aligned} \tag{89}
$$

Therefore, computing derivatives of the solution does not cause any new technical problem.

Special Case $|1 - z_i| \ll 1$ at Some Node K_i, $i \in [1, n_j]$

Without loss of generality suppose that $z_i = 1 - \epsilon$ and $z_{i+1} \gg 1 + \epsilon$ with $0 < \epsilon \ll 1$. The other case $z_i = 1 + \epsilon$ and $z_{i-1} \ll 1 - \epsilon$ could be treated similarly. Then, let

us introduce a ghost point K_* such that $z_* = 1 + \epsilon$. So at the interval $[K_i, K_*]$, we will use the numerically stable solution in Equation 65; while at the interval $[K_*, K_{i+1}]$, we will use the regular solution in Equation 63.

Since K_* is the ghost point, we do not have a market quote available at K_*. All we can say is that we still assume the local variance/volatility to be a piecewise linear function of K at $[K_*, K_{i+1}]$ and $[K_i, K_*]$. It has to be continuous but with a possible jump in skew at K_*.

Since a market quote at K_* is not available, we can replace it with any reasonable value. For instance, an interpolated value between market quotes at K_i, K_{i+1} obtained by using no-arbitrage interpolation could be used.[5] Then we obtain four equations for $C^{(1)}_{j,*}, C^{(2)}_{j,*}, \upsilon^0_{j,*} \upsilon^1_{j,*}$:

$$\begin{aligned} P_i(x)\Big|_{x=x_i} &= P_*(x)\Big|_{x=x_i}, \\ P_*(x)\Big|_{x=x_*} &= P_{interp}(x)\Big|_{x=x_*}, \\ \frac{\partial P_*(x)}{\partial x}\Big|_{x=x_i} &= \frac{\partial P_i(x)}{\partial x}\Big|_{x=x_i}, \\ \upsilon^0_{j,i} + \upsilon^1_{j,i} x_* &= \upsilon^0_{j,*} + \upsilon^1_{j,*} x_*, \quad i = 1, \ldots, n_j. \end{aligned} \tag{90}$$

which should be added to Equation 88. Solving this new combined linear system in the same way as we did for Equation 88, we find the values of all unknown $C^{(1)}_{j,i}, C^{(2)}_{j,i}, \nu^0_{j,i}, \nu^1_{j,i}$ where now $i \in \{[1, n_j] \cup *\}$.

DISCUSSION

First, let us mention that in many practical calculations, either coefficients $a_2 = \nu^1_{j,i}$ at some i, or $b_2 = \nu^0_{j,i}$, $a_2 = \nu^1_{j,i}$ (see, for instance, Equation 57) are small. Of course, in that case the general solution of Equation 63 remains valid. However, when computing the values of hypergeometric functions numerically, the errors grow significantly in such a case. This outcome is especially pronounced when computing the source term integral I_{12}. The main point is that either the hypergeometric function takes a very small value, and then the constants $C^{(1)}_{j,i}$, $C^{(2)}_{j,i}$ should be very large to compensate, or vice versa. The resolution of this issue requires high-precision arithmetic, and what is more important, it requires taking into account many terms in a series representation of the hypergeometric functions, which significantly slows down the total performance of the method.

To eliminate those problems we can look at asymptotic solutions of Equation 57, taking into account the existence of small parameters from the very beginning. This approach was successfully elaborated on in Itkin and Lipton (2018) and Carr and Itkin (2018), so we do not describe it here in detail.

In Carr and Itkin (2018) we calibrated the ELVG model, for example, to the data set taken from Balaraman (2016). In that article an implied volatility surface of the S&P 500 was presented, and the local volatility surface was constructed using the Dupire formula. We took data for the first 12 maturities and all strikes as they are given in Balaraman (2016). Our results demonstrated the high accuracy and speed of the calibration.

When doing so, a technical note should be made. We mentioned previously that in our model for every term the slopes of the smile at strikes close to zero, $\nu^1_{j,0}$, and infinity, ν^1_{j,n_j}, are free parameters of the model. So, often traders have an intuition about those values. However, in our numerical experiments we set them up using just some plausible test values. In particular, in Carr and Itkin (2018) for the sake of simplicity, for all smiles we used $\nu^1_{j,0} = -0.3$, and $\nu^1_{j,n_j} = 0.1$. Accordingly, for the instantaneous variance $\nu_j(x_i) = p_j(\nu^0_{j,i} + \nu^1_{j,i} \log(x_i))/2$, the slopes at both zero and plus infinity are time dependent and can be computed by using this definition.

As a numerical solver for the system of linear equations, we used the standard MATLAB *fsolve* function and employed a "trust-region-dogleg" algorithm. Parameter "TypicalX" has to be chosen carefully to speed up calculations.

In this article we repeated that test, but now using the GLVG instead of the ELVG. The results look the same as in Figure 5 of Carr and Itkin (2018), that is, the quality of the fit is the same, and the performance of the method is almost the same. But the conclusion of Carr and Itkin (2018) remains intact, namely, that the performance of this model is much better than that reported in both Itkin (2015) and Itkin and Lipton (2018).

Therefore, a natural question would be, which flavor of the LVG model—arithmetic or geometric—is preferable? Perhaps, if the ultimate goal is fast calibration of the given smile, both could be used interchangeably, and both are capable of providing a good and fast

[5] Although it looks attractive, we cannot require $\nu^1_{j,i} = \nu^1_{j,*}$ since this also gives rise to $\nu^0_{j,i} = \nu^0_{j,*}$. However, $\nu^0_{j,i}$ changes sign at $z = 1$.

fit. However, for modeling option prices the difference between the geometric and arithmetic LVG models is of the same kind as between the Bachelier and Black–Scholes models. So, for instance, for modeling stock prices, the latter would be preferable; while for modeling interest rates, the former could provide negative values, which nowadays is a desirable feature.

CONCLUSIONS

In this article we propose another flavor of the local variance gamma (LVG). Several contributions are made as compared with the existing literature. First, the model is constructed on the basis of a gamma time-changed *geometric* Brownian motion with drift, while in all previous articles, an arithmetic Brownian motion was used.

Second, we consider two models of the local variance—piecewise linear in strike and piecewise linear in the log-strike, and the model of the local volatility piecewise linear in strike (which is new in this context). We also consider a combined model of the local variance, which is piecewise linear in strike in the internal intervals and linear in the log-strike at the first and last intervals (see below for more detail).

Third, we show that for all these new constructions it is still possible to derive an ODE for the option price, which plays the role of Dupire's equation for the standard local volatility model. Moreover, it can be solved in closed form in terms of various flavors of hypergeometric functions. For doing so we propose several new versions of no-arbitrage interpolation, similar to how this was done in Carr and Itkin (2018) but in a slightly different form, so the entire approach becomes tractable.

Also we shortly discuss various asymptotic solutions that allow a significant acceleration of the numerical solver and improvement of its accuracy in those cases (i.e., when parameters of the model obey the conditions to apply the corresponding asymptotic). For the sake of brevity we omit the exact derivations as they can be obtained in a way similar to that in Carr and Itkin (2018).

Fourth, new boundary conditions are derived for the put option in the GLVG. They are discrete and converge to the standard boundary conditions in the continuous case (Dupire). These conditions are constructed using some analog of discrete compounding, which is natural for the LVG model.

And finally, we notice that for any piecewise model of the local variance/volatility at edge intervals where strikes are close either to 0 or to infinity, one has to switch to the local variance linear in log-strike because of Roger Lee's moment formula. Thus, the whole local variance/volatility model becomes a combination of the original model at the internal intervals and local variance linear in log-strike at the edge intervals.

The other features of the GLVG model are pretty much inherited from the ELVG. For instance, similar to in Carr and Itkin (2018), we show that given multiple smiles the whole local variance/volatility surface can be recovered without having to solve any optimization problem. Instead, it can be done term-by-term by solving a system of nonlinear algebraic equations for each maturity, which is a faster method.

APPENDIX A

NUMERICALLY SATISFACTORY SOLUTIONS OF EQUATION 59 AT $\mathcal{X} \to \infty$

According to Olver (1997), the numerically satisfactory fundamental solutions of Equation 59 in the vicinity of **singularity at $z = \infty$** are

$$\begin{aligned} y_1(x) &= z^m[z^{-A}{}_2F_1(A, A-C+1, A-B+1, 1/z)], \\ y_2(x) &= z^m[z^{-B}{}_2F_1(B, B-C+1, B-A+1; 1/z)], \end{aligned} \tag{A1}$$

where in our case $A = m - 1$, $B = m$, $C = c$. This substitution transforms the second solution in Equation A.1 to

$$y_2(x) = z^m[z^{-m}{}_2F_1(m, m-c+1, 2; 1/z)], \tag{A2}$$

and behaves well at $z \to \infty$. However, since in our setting $n \equiv A - B + 1 = m - 1 - m + 1 = 0$, and due to the property

$$\begin{aligned} \lim_{c\to -n} \frac{F(a,b,c;z)}{\Gamma(c)} &= \frac{(a)_{n+1}(b)_{n+1}}{(n+1)!} z^{n+1} F(a+n+1, b+n+1, n+2; z), \\ y_1(x) &= F(m-1, m-c, 0; z) \\ &= \Gamma(0)\frac{(m-1)_1(m-c)_1}{(1)!} z F(m, m-c+1, 2; z), \end{aligned}$$

it becomes apparent that the first solution differs from the second by just a constant multiplier, that is, they are not independent. Therefore, in this case instead the first solution

$\gamma_1(x)$ should be chosen based on a more sophisticated analytic continuation of the Hypergeometric function, Bateman and Erdélyi (1953).

$$\gamma_1(x) = z^m[(-z)^{1-m}\frac{\Gamma(c)}{\Gamma(m)\Gamma(c-m+1)}\Psi(z)], |z|>1, |\mathrm{ph}(-z)|<\pi,$$
$$\Psi(z) = 1-\frac{1}{z}\sum_{k=0}^{\infty}\frac{(m-1)_{k+1}(m-c)_{k+1}}{k!(k+1)!}z^{-k}[\log(-z)+\phi_k],$$
$$\phi_k \equiv \psi(k+1)+\psi(k+2)-\psi(m+k)-\psi(c-m-k),$$
$$(m)_k = \Gamma(m)/\Gamma(k), \quad \psi(x) = \Gamma'(x)/\Gamma(x). \tag{A3}$$

APPENDIX B

NO-ARBITRAGE INTERPOLATION AT $\mathcal{X}\to\infty$

In this Appendix we prove the following Proposition:

Proposition 1. *Recall that according to Equation 78 the proposed interpolation scheme for $V(\chi, T_{j-1}, S)$ at the interval $x_{n_j} \le x \le \infty$ reads*

$$c(\chi) = V(\chi, T_{j-1}, S) = \gamma_\infty z^{-\nu}, \quad z = \chi + \frac{b_2}{a_2}, \tag{B1}$$

where $\gamma_\infty > 0, \nu > 0$ are some constants determined below in the proof. Also this scheme preserves no-arbitrage.

Proof By construction, at $K\to\infty, c(\chi)$ converges to the correct boundary condition, that is, vanishes. Assuming that K_{n_j} is in-the-money, Equation 78 can be rewritten in the form

$$P(K) = A(T_{j-1})K - B(T_{j-1})S + \gamma_\infty[\log(K/S)+b_2/a_2]^{-\nu}. \tag{B2}$$

As at this interval $\nu = b_2 + a_2\log(K/S) > 0$, and it was assumed that $K > S$, we must have $a_2 > 0$. Accordingly, to have a positive put price we require $\gamma_\infty > 0$. This constant could be determined by using a known put value at K_{n_j}, that is, $P(K_{n_j}) = P_{n_j}$. This yields

$$\gamma_\infty = [P_{n_j} - A(T_{j-1})K_{n_j} - B(T_{j-1})S]\left[\frac{b_2}{a_2}+\log\left(\frac{K_{n_j}}{S}\right)\right]^{\nu} > 0. \tag{B3}$$

Therefore, this definition is also consistent with the requirement of positiveness of γ_∞.

As this is described in detail in Itkin and Lipton (2018), the no-arbitrage conditions for the put price read

$$P>0, \quad P_K>0, \quad P_{K,K}>0.$$

Differentiating Equation B.2 on K, and then again, we obtain

$$P'_K = A(T_{j-1}) - \frac{\gamma_\infty\nu}{K}\left[\frac{b_2}{a_2}+\log\left(\frac{K}{S}\right)\right]^{-1-\nu},$$
$$P''_K = \frac{\gamma_\infty\nu}{a_2K^2}\left[\frac{b_2}{a_2}+\log\left(\frac{K}{S}\right)\right]^{-\nu-2}[b_2 + a_2(1+\nu+\log(K/S))]. \tag{B4}$$

Analyzing these expressions we conclude that $P''_K > 0$. Observe that at $K\to\infty$ we also have $P'_K > 0$. Also observe that P'_K is a monotone function of K. Therefore, let us look at $P'_K(K_{n_j})$. Substitution of $K = K_{n_j}$ into the first line of Equation B.4 yields

$$P'_K(K_{n_j}) = A(T_{j-1}) + \frac{a_2\nu}{K_{n_j}(b_2+a_2\log(K/S))}[A(T_{j-1})K_{n_j} - B(T_{j-1})S - P_{n_j}]. \tag{B5}$$

As the put value exceeds its intrinsic value, $P'_K(K_{n_j})$ is positive if

$$0 < \nu < A(T_{j-1})K_{n_j}\left[\frac{b_2}{a_2}+\log\left(\frac{K_{n_j}}{S}\right)\right]$$
$$[P_{n_j} - A(T_{j-1})K_{n_j} + B(T_{j-1})S]^{-1} \equiv \Omega. \tag{B6}$$

At large K_{n_j} the expression in the first square brackets is large, and in the second ones–small. Thus the upper boundary for ν is high enough.

Finally, we take into account the well-known upper bound of the put option price, which is (Hull 1997)

$$P_{n_j} \le A(T_j)K_{n_j}.$$

Because of that, we can rewrite Equation B6 as

$$0 < \nu < \frac{A(T_{j-1})}{B(T_{j-1})}\frac{K_{n_j}}{S}\left[\frac{b_2}{a_2}+\log\left(\frac{K_{n_j}}{S}\right)\right]$$
$$\approx \frac{K_{n_j}}{S}\left[\frac{b_2}{a_2}+\log\left(\frac{K_{n_j}}{S}\right)\right] \le \Omega. \tag{B7}$$

Therefore, if ν is chosen according to Equation B.6 or Equation B7, this guarantees that $P'_K(K_{n_j}) > 0$. As $P'_K(K)$ is a monotone function of K, this proves that with this choice of ν the condition $P'_K(K) > 0$ is valid at the whole interval $x_{n_j} \le x < \infty$. Thus, this interpolation preserves no-arbitrage. ■

APPENDIX C

NO-ARBITRAGE INTERPOLATION AT $\mathcal{X} \to \infty$

In this Appendix we prove the following Proposition:

Proposition 2. *Recall that according to Equation 78 the proposed interpolation scheme for $V(\chi, T_{j-1}, S)$ at the interval $-\infty \le x < x_1$ reads*

$$V(\chi, T_{j-1}, S) = \omega_0 e^z / z, \quad z = \chi + \frac{b_2}{a_2}, \tag{C1}$$

where $\omega_0 = V(\chi_1, T_{j-1}, S) z_1 e^{-z_1} < 0$ is constant. Also this scheme preserves no-arbitrage.

Proof Obviously, at $K = K_1$ we have $\chi_1 = \log(K_1/S)$, $V(\chi, T_{j-1}, S) = V(\chi_1, T_{j-1}, S) \equiv V_1$, therefore, assuming the strike K_1 is out of the money

$$\omega_0 = V_1 z_1 e^{-z_1} < 0. \tag{C2}$$

As this is described in detail in Itkin and Lipton (2018), the no-arbitrage conditions for the put price read

$$P > 0, \quad P_K > 0, \quad P_{K,K} > 0.$$

Based on Equation 78 and the definition of V in Equation 45, the put price at this interval can be represented as

$$P(K, T_{j-1}, S) = \omega_0 e^z / z = \omega_0 e^{b_2/a_2} \frac{K/S}{\log(K/S) + b_2/a_2}. \tag{C3}$$

As at this interval $v = b_2 + a_2 \log(K/S)$, and it was assumed that $K < S$, we must have $a_2 < 0$. Accordingly, to have a positive put price we require $\omega_0 < 0$. This is consistent with the value of ω_0 introduced in Equation C2).

Differentiating Equation C3 on K, and then again, we obtain

$$\begin{aligned} P'_K &= \frac{\omega_0 a_2}{S} e^{b_2/a_2} \frac{b_2 - a_2 + a_2 \log(K/S)}{(b_2 + a_2 \log(K/S))^2} > 0, \\ P''_K &= -\omega_0 \frac{a_2^2}{KS} e^{b_2/a_2} \frac{b_2 - 2a_2 + a_2 \log(K/S)}{(b_2 + a_2 \log(K/S))^3} > 0. \end{aligned} \tag{C4}$$

Thus, the proposed scheme can be used for interpolation because it provides correct put option prices at $K = K_1$ and $K \to 0$, and is monotone in K. Moreover, it preserves no-arbitrage.

■

APPENDIX D

NO-ARBITRAGE INTERPOLATION AT $\mathcal{X} \to 1$

As by definition in Equation 63 $z = -\frac{a_2}{b_2} x$, this implies that

$$1 - z = 1 + \frac{a_2}{b_2} x = \frac{v_{ji}}{b_2}.$$

Obviously, $v_{ji} \ge 0$. Therefore, when z is close to 1 two situations are possible:

1. $z < 1$, which implies $b_2 > 0$, and accordingly $a_2 < 0$;
2. $z > 1$, which implies $b_2 < 0$, and accordingly $a_2 > 0$.

Suppose for interpolation of the put price we use Equation 73, that is,

$$\begin{aligned} P(x) &= \gamma_0 + \gamma_2 x^2, \quad x_1 \le x \le x_3, \\ \gamma_0 &= \frac{P(x_3)x_1^2 - P(x_1)x_3^2}{x_1^2 - x_3^2} = P_1 - \frac{P_3 - P_1}{x_3^2 - x_1^2} x_1^2 > 0, \\ \gamma 2 &= \frac{P(x_1) - P(x_3)}{x_1^2 - x_3^2} > 0. \end{aligned} \tag{D1}$$

The second inequality is obvious since $P(x_3) > P(x_1)$ if $x_3 > x_1$. The first one follows from the fact that the put price exceeds its intrinsic value, that is,

$$P_i = [A(T_j)K_i - B(T_j)S]^+ + \varepsilon_i, \quad \varepsilon_i > 0.$$

Suppose, for example, that both strikes K_1, K_3 are in-the-money. Then

$$\begin{aligned} \gamma_0 &= P_1 - \frac{P_3 - P_1}{x_3^2 - x_1^2} x_1^2 = P_1 - \frac{A(T_j)S(x_3 - x_1) + (\varepsilon_3 - \varepsilon_1)}{x_3^2 - x_1^2} x_1^2 \\ &= \frac{P_1 x_3 + x_1(P_1 - A(T_j)K_1)}{x_3 + x_1} + \frac{\varepsilon_1 - \varepsilon_3}{x_3^2 - x_1^2} x_1^2 > 0, \end{aligned} \tag{D2}$$

as based on the properties of the put price $\varepsilon_1 > \varepsilon_3$.

From Equation D.1 it follows that

$$\begin{aligned} V &= \gamma_0 + \gamma_2 x^2 - A(T_j)Sx + B(T_j)S = \overline{\gamma}_0 + \gamma_1 z + \overline{\gamma}_2 z^2, \\ \overline{\gamma}_0 &= \gamma_0 + + B(T_j)S, \quad \gamma_1 = \frac{a_2}{b_2} A(T_j)S, \quad \overline{\gamma}_2 = \gamma_2 \frac{a_2^2}{b_2^2}. \end{aligned} \tag{D3}$$

It was proven in Carr and Itkin (2018) that interpolation Equation D1 preserves no-arbitrage, and so that in Equation D3. We use it when computing $J_2(x)$ in Equation 84.

ACKNOWLEDGMENT

We thank an anonymous referee for very useful comments.

REFERENCES

Abramowitz, M., and I. Stegun. *Handbook of Mathematical Functions*. Mineola, NY: Dover Publications. 1964.

Askey, R., and A. B. O. Daalhuis. "Generalized Hypergeometric Function." In *NIST Handbook of Mathematical Functions*, edited by F. Olver, D. Lozier, R., Boisvert, and C. Clark. Cambridge, UK: Cambridge University Press. 2010.

Balaraman, G. 2016. "Modeling Volatility Smile and Heston Model Calibration Using QuantLib Python." http://gouthamanbalaraman.com/blog/volatility-smile-heston-model-calibration-quantlib-python.html.

Bateman, H., and A. Erdélyi. *Higher Transcendental Functions*, vol. 1. Bateman Manuscript Project California Institute of Technology. New York: McGraw-Hill. 1953.

Bergomi, L. *Stochastic Volatility Modeling*. CRC Financial Mathematics Series. London: Chapman and Hall. 2016.

Bochner, S. 1949. "Diffusion Equation and Stochastic Processes." In *Proceedings of the National Academy of Sciences*, 368–370.

Carr, P., and A. Itkin. 2018. "An Expanded Local Variance Gamma Model." https://arxiv.org/abs/1802.09611.

Carr, P., and S. Nadtochiy. 2014. "Local Variance Gamma and Explicit Calibration to Option Prices." https://arxiv.org/abs/1308.2326.

Carr, P., and S. Nadtochiy. 2017. "Local Variance Gamma and Explicit Calibration to Option Prices." *Finance* 27: 151–193.

Coleman, T., Y. Kim, Y. Li, and A. Verma. 2001. "Dynamic Hedging with a Deterministic Local Volatility Function Model." *The Journal of Risk* 4: 63–89.

De Marco, S., P. Friz, and S. Gerhold. 2013. "Rational Shapes of Local Volatility." *Risk* 2: 82–87.

Derman, E., and I. Kani. 1994. "Riding on a Smile." *Risk* 7 (2): 32–39.

Dupire, B. 1994. "Pricing with a Smile." *Risk* 7: 18–20.

Ekström, E., and J. Tysk. 2012. "Dupire's Equation for Bubbles." *International Journal of Theoretical and Applied Finance* 15 (6).

Gatheral, J. 2006. *The Volatility Surface*. Wiley Finance.

Gerhold, S., and P. Friz. 2015. "Extrapolation Analytics for Dupire's Local Volatility." In *Large Deviations and Asymptotic Methods in Finance,* 273–286. Vol. 110, *Springer Proceedings in Mathematics & Statistics*. Berlin: Springer.

Hull, J., and A. White. 2015. "A Generalized Procedure for Building Trees for the Short Rate and Its Application to Determining Market Implied Volatility Functions." *Quantitative Finance* 15: 443–454.

Hull, J. C. *Options, Futures, and Other Derivative Securities*, 3rd ed. Upper Saddle River, NJ: Prentice-Hall. 1997.

Itkin, A. 2015. "To Sigmoid-Based Functional Description of the Volatility Smile." *North American Journal of Economics and Finance* 31: 264–291.

Itkin, A., and A. Lipton. 2018. "Filling the Gaps Smoothly." *Journal of Computational Sciences* 24: 195–208.

Kienitz, J., and P. Caspers. *Interest Rate Derivatives Explained: Term Structure and Volatility Modelling*. Vol. 2, *Financial Engineering Explained*, 1st ed. London: Palgrave Macmillan UK. 2017.

Kienitz, J., and D. Wetterau. *Financial Modelling: Theory, Implementation and Practice with MATLAB Source*. The Wiley Finance Series. Hoboken, NJ: Wiley. 2012.

Lee, R. 2004. "The Moment Formula for Implied Volatility at Extreme Strikes." *Mathematical Finance* 14: 469–480.

Lipton, A. *Mathematical Methods for Foreign Exchange: A Financial Engineer's Approach*. Singapore: World Scientific. 2001.

Lipton, A., and A. Sepp. "Credit Value Adjustment in the Extended Structural Default Model." In *The Oxford Handbook of Credit Derivatives*, 406–463. Oxford, England: Oxford University Press. 2011.

Lörinczi, J., F. Hiroshima, and V. Betz. "Feynman–Kac-Type Theorems and Gibbs Measures on Path Space." No. 34 in *De Gruyter Studies in Mathematics*. Berlin/Boston: Walter de Gruyter GmbH & Co. 2011.

Ng, E., and M. Geller. 1970. "On Some Indefinite Integrals of Confluent Hypergeometric Functions." *Journal of Research of the National Bureau of Standards*. Section B: *Mathematical Sciences* 748: 85–98.

Olver, F. *Asymptotics and Special Functions*. AKP Classics. A K Peters/CRC Press. 1997.

Polyanin, A., and V. Zaitsev. *Handbook of Exact Solutions for Ordinary Differential Equations*, 2nd ed. Boca Raton, FL; London; New York; Washington, D.C.: CRC Press Company. 2003.

Revuz, D., and M. Yor. *Continuous Martingales and Brownian Motion*, 3rd ed. Berlin: Springer. 1999.

Shreve, S. 1992. "Martingales and the Theory of Capital-Asset Pricing." *Lecture Notes in Control and Information Sciences* 180: 809–823.

Vasil'eva, A., V. Butuzov, and L. Kalachov. "The Boundary Function Method for Singular Perturbation Problems." *Studies in Applied Mathematics*. Philadelphia, PA: SIAM. 1995.

ADDITIONAL READING

An Empirical Examination of the Relation between the Option-Implied Volatility Smile and Heterogeneous Beliefs

Shu Feng, Xiaoling Pu, and Yi Zhang
The Journal of Derivatives
https://jod.pm-research.com/content/25/4/36

ABSTRACT: *An option contract is a zero-sum game, so two identical risk-averse investors would never take opposite sides of it. While they will agree on the correct option price, they would never trade with each other. Heterogeneity is essential for options trading to exist, and aggregating diverse expectations into a single market clearing price is an important function of any derivatives market. In this article, the authors look at the impact of heterogeneous beliefs about earnings, as reflected in the dispersion of analysts' forecasts in the IBES database. The effect on the market is measured by the slopes of the volatility smile for out-of-the-money (OTM) minus at-the-money (ATM) puts (left side of the smile) and OTM minus ATM calls (right side). Smiles for individual stocks are higher and more smile-shaped than for the SPX index and show significant and interesting effects from the explanatory variables, including firm size, liquidity, market volatility, and book-to-market. But controlling for those effects, dispersion in earnings forecasts raises OTM IVs relative to ATM IVs, both in regressions and in portfolio sorts. Interesting differences appear between systematic and idiosyncratic components of the smile slope, with systematic effects especially important for OTM puts, while OTM calls are more influenced by the idiosyncratic component.*

Towards a General Local Volatility Model for All Asset Classes

Dariusz Gatarek and Juliusz Jabłecki
The Journal of Derivatives
https://jod.pm-research.com/content/27/1/14

ABSTRACT: *The authors propose a unified approach to local volatility modeling, encompassing all asset classes, with straightforward application to equity and interest rate underlyings. Specifically, they consider a local volatility model for asset-for-asset or Margrabe (1978) options under general conditions that underlying dynamics follow Itô processes and derive a closed-form non-parametric local volatility formula. They then show that many standard contracts—European equity, FX, and interest rate options—can be seen as particular examples of the Margrabe-type payoff, which allows them to analyze equity and interest rate instruments, for example, as special cases of the same general local volatility model, rather than two separate models. They then derive a Markovian projection for the general model, with an approximate local volatility diffusion for the Margrabe option underlying. Finally, they discuss a specific application of the model to swaptions qua asset-for-asset options, where they consider the Markovian projection with some frozen parameters as a minimal "poor man's" model, featuring equity-like dynamics for the swap rate with its own "short rate" and the "dividend" implied from the term structure of interest rates. Using a number of numerical examples, they compare the minimal model to a fully fledged Cheyette local volatility model and the market benchmark Hull–White one-factor model (Hull and White 1990), demonstrating the adequacy of the "poor man's" model for pricing European and Bermudan payoffs.*

Quadrinomial Trees to Value Options in Stochastic Volatility Models

Julián A. Pareja-Vasseur and Freddy H. Marín-Sánchez
The Journal of Derivatives
https://jod.pm-research.com/content/27/1/49

ABSTRACT: *This article describes in detail the multiplicative quadrinomial tree numerical method with nonconstant volatility, based on a system of stochastic differential equations of the GARCH-diffusion type. The methodology allowed for the derivation of the first two moments of the proposed equations to estimate the respective recombination between discrete and continuous processes and, as a result, a numerical methodological proposal is formally presented to value, with relative ease, both real and financial options, when the volatility is stochastic. The main findings showed that in the proposed method, when volatility approaches zero, the multiplicative binomial traditional method is a particular case, and the results are comparable between these methodologies, as well as to the exact solution offered by the Black–Scholes model. Finally, the originality of the methodological proposal is that it allows for the emulation in a simple way of the presence of a nonconstant volatility in the price of the underlying asset, and it can be used to value all kinds of options both in the real world and in risk-neutral situations.*